Harman Ciaran J. (Orcid ID: 0000-0002-3185-002X)
Hobbs Benjamin F. (Orcid ID: 0000-0003-1783-3597)
Sivapalan Murugesu (Orcid ID: 0000-0003-3004-3530)

Assessment of climate, sizing, and location controls on green infrastructure efficacy: A timescale framework

F. Hung[1], C. J. Harman[2*], B. F. Hobbs[2], and M. Sivapalan[3,4]

[1]Department of Civil and Environmental Engineering, Lehigh University, PA, USA

[2]Department of Environmental Health and Engineering, Johns Hopkins University, MD, USA

[3]Department of Civil and Environmental Engineering, University of Illinois at Urbana-Champaign, IL, USA

[4]Department of Geography and Geographic Information Science, University of Illinois at Urbana-Champaign, IL, USA

Corresponding author: Ciaran Harman (charman1@jhu.edu)

Key Points:

- The ability of GI to mitigate peak discharge depends on the climate and sewershed characteristics, as well as its design
- We propose a simple framework for capturing these controls in terms of timescales and three dimensionless numbers
- GI efficacy in treating CSO volume and frequency may depend on the precipitation pattern and the location of GI within a sewershed

This article has been accepted for publication and undergone full peer review but has not been through the copyediting, typesetting, pagination and proofreading process which may lead to differences between this version and the Version of Record. Please cite this article as doi: 10.1029/2019WR026141

Abstract

We investigate how the effectiveness of green infrastructure (GI) to mitigate the frequency and magnitude of significant discharge events and Combined Sewer Overflows (CSOs) depend on both climate and sewershed characteristics and propose a theoretical framework for a holistic assessment of GI's efficacy. The framework is based on the comparison of three characteristic timescales that control the production of peak discharge: rainfall duration (t_r), travel time in the sewer network (t_n), and the duration of rain that would be required to fill the GI's storage (t_{GI}). Storm events can then be characterized by two ratios of these timescales: $T_n = t_n/t_{GI}$ and $T_r = t_r/t_{GI}$. A third dimensionless number characterizes critical storms during which adverse events (such as CSOs) occur, and allows us to identify the combinations of T_n and T_r for which GI may substantially mitigate those events. The results of numerical experiments with the model demonstrate that the storms for which GI can substantially reduce peak discharge and CSO volume typically occur in a narrow band of T_n and T_r. Within that band, the efficacy of GI may depend on the location of GI within the sewershed if network routing substantially affects the timing and magnitude of flood peaks. The proposed framework is applied to examine the efficacy of GI using historical precipitation data from two major US cities: Philadelphia, PA and Seattle, WA, and the results of this comparative analysis suggest that GI location is an important control on catchment-scale GI efficacy in Philadelphia, but less so in Seattle.

Plain Language Summary

Combined sewer overflows (CSO) occur when storm rainfall exceeds the capacity of the sewer system to drain it. Green infrastructure (GI) is intended to mitigate the occurrence and severity of CSOs. But how effective will it be in helping to manage CSOs? Here we present a theoretical framework to address this question, by focusing on the major physical controls on the efficacy of GI for managing CSOs, including the relative roles of climate, the size of the sewershed, and the location of the GI within it. The framework is based on three characteristic timescales: storm duration, travel time to the overflow location, and time required to fill GI storage. We use the framework to explore how GI might work differently in different places. The results show that GI is most effective under certain combinations of climate and sewershed conditions, and that the location of GI within the sewershed can be very critical. The latter effect was found to be more evident, for example, in Philadelphia, PA, than in Seattle, WA, due to differences in storm duration and intensity between these two places. In these ways, the proposed framework can support green infrastructure planning by providing insights on location-effectiveness tradeoffs.

1. Introduction

Urbanization has changed the hydrological response of watersheds in which impervious areas and the drainage system expedite the movement of stormwater runoff to the watershed outlet, and causes water quantity and quality problems in adjacent water bodies (Barbosa et al., 2012; Lucas & Sample, 2015; Tavakol-Davani et al., 2016). These problems are exacerbated in cities that experience combined sewer overflows (CSOs). A combined sewer system is a sewer network that collects residential sewage, industrial wastewater, and stormwater. A CSO occurs when the volume of stormwater entering the combined sewer system during a storm event such that the combined flow exceeds the system's capacity, leading to the release of untreated wastewater into receiving waters. The resulting discharges of untreated wastewater and stormwater degrade water quality and can prevent beneficial uses of water for days (Lau et al., 2002; Mailhot et al., 2015; Pálfy et al., 2016). In the United States, combined sewer systems serve about 40 million people in approximately 772 communities (USEPA, 2011).

Traditional approaches to stormwater management emphasize the so-called "gray infrastructure," which consists of structural measures (e.g., underground storage tunnels) to control stormwater runoff and pollution. These approaches usually have limited flexibility to adapt to future development and the changing climate. In contrast, green infrastructure (GI) uses distributed systems that mimic the hydrological functions of a natural watershed to retain, infiltrate, and evaporate stormwater to reduce runoff and pollution, and can be implemented incrementally to adapt to future changes (Barbosa et al., 2012; Chocat et al., 2007; Kong et al., 2017). However, due to the complex process of CSO generation, the efficacy of GI in reducing stormwater is highly uncertain and may depend on many factors, including the capacity of sewer systems, GI storage and infiltration capacity, and storm intensity and duration.

Recent reviews have synthesized the GI effects at local and catchment scales and pointed out the challenges of their assessment. Modeling studies often lack data for parameterization and calibration and are infeasible for more sizable watersheds, while monitoring studies face challenges of experimental design (lack of long-term and consistent data and proper reference catchments for comparison) and various confounding factors preventing the detection of GI effects at catchment scale (Golden & Hoghooghi, 2018; Jefferson et al., 2017; Li et al., 2017).

Despite the efforts in the GI literature to explore factors that influence GI efficacy in reducing storm runoff volume and peak discharge (Bell et al., 2016; Jarden et al., 2016; Lim & Welty, 2017; Pennino et al., 2016; Shuster & Rhea, 2013), there is still a lack of methods to efficiently evaluate whether these reductions will translate into CSO volume and frequency reduction at the catchment outlet. As stormwater management metrics, CSO volume represents the pollution level whereas CSO frequency indicates the potential disturbance of beneficial water uses (Andrés-Doménech et al., 2010; Lau et al., 2002); both are particularly important if the purpose of GI is to control CSOs. Below, we summarize GI studies that focus on CSOs.

Schroeder et al. (2011) compared the CSO frequency and the minimum CSO-generating rainfall volume estimated from statistical analysis in four sewersheds in Berlin, Germany. They show that the sewershed with GI exhibits a higher minimum CSO threshold (9.7 mm; 4.7 mm in the other three sewersheds) and a lower CSO frequency (13 CSOs/yr; others range from 34 to 36 CSOs/yr). Similarly, Pennino et al. (2016) investigated the statistical relationship between GI installation and CSO metrics (frequency, volume, and duration) derived from monitoring data in Washington, DC, US, and found that the CSO metrics are consistently lower in sewersheds with GI, although not statistically significant. Fu et al. (2019) developed a scenario-based simulation tool to assess what combination of GIs and how much installations are needed to eliminate a CSO generated by a two-year storm event. They concluded that GIs alone could not entirely remove the CSO unless gray infrastructure with substantial storage was added to

the system. Jean et al. (2018) compared modeling and rainfall data selection methods for the estimation of the CSO volume reduction needed to achieve the CSO frequency control target and suggested continuous simulations over event-based simulations.

Another group of studies applied hydrological modeling to compare GI with traditional gray infrastructure. For example, Tavakol-Davani et al. (2016) evaluated climate change impacts on rain-harvesting system efficacy on CSO control and reported that the rain-harvesting systems are more effective in reducing CSO frequency than CSO volume and duration under the intense climate change scenario. Lucas & Sample (2015) compared GI with and without outlet control in managing CSOs together with gray infrastructure (tunnel storage) and showed that GI with outlet control performs better than gray infrastructure in reducing CSO volume but not as well in controlling CSO frequency. Casal-Campos et al. (2015) investigated the robustness of several gray and green infrastructure strategies considering CSO volume, costs, flood risks, water quality, and greenhouse emissions and concluded that sewer system retrofit might be most effective in treating CSOs, but GI strategies perform relatively well in every category and, therefore, are more robust.

Based on the findings in the literature, we believe that sewer overflows are not only a function of the volume of runoff and the sewer capacity, but also climate and landscape factors that control the timing of flood wave arrival at the location of interest. However, systematic methods and a theoretically based framework for evaluating GI efficacy are still missing in the literature.

Theoretical frameworks for understanding the effects of runoff timing on flood peaks that integrate climate and hydrological variability at watershed scales have been developed since the late 1980s (Reggiani et al., 2000; Robinson & Sivapalan, 1997; Wood & Hebson, 1986; Woods & Sivapalan, 1999). Recently, new frameworks have been proposed that attempt to quantify the catchment response to rainfalls from a holistic view while addressing temporal and spatial heterogeneity (Jothityangkoon & Sivapalan, 2009; Seo et al., 2012; Troch et al., 2009; Wagener et al., 2007, 2010). For example, Robinson & Sivapalan (1997) demonstrated how key elements of the hydrological response of a watershed are determined by the timescales involved (e.g., storm duration, catchment response time, and time between storms). Similarly, Seo et al. (2012) illustrated the effects of storm movement on peak discharge.

Inspired by the work by Robinson & Sivapalan (1997), we propose here a new framework for assessing the potential of GI to reduce peak discharges and CSOs. This is done by augmenting Robinson & Sivapalan's framework with timescales associated with climate, sewershed, and GI interactions, in which GI is viewed as an integrated storage and infiltration system. More specifically, our focus is to develop a theoretical framework based on the timescales to identify the mechanisms dominating the CSO generating process in urban sewersheds. A sewershed is a delineation of the land area contributing stormwater and wastewater to a single downstream point within a sewer system. This theoretical framework has the advantage of needing less data and model calibration compared to traditional highly parameterized models and, therefore, is suitable for applications in sizable sewersheds. The key questions addressed in this paper are:

(1) What are the key attributes of the climate and sewersheds that affect GI efficacy in reducing peak runoff, CSO volume, and CSO frequency?

(2) For what types of storms will GI have an appreciable effect on CSOs?

The theoretical framework presented here is intended to improve understanding of the peak discharge and CSO generating mechanisms and how they depend on precipitation patterns,

sewershed characteristics, and GI. This understanding can help identify situations where certain hydrological characteristics dominate CSO generating processes and therefore provide guidance for managing CSOs and implementing GI.

The remainder of this paper is organized as follows. In Section 2, we introduce the timescales, the proposed GI-based CSO management framework, and a dimensionless number that represents the lower bounds for CSO-producing storms. Then, in Section 3, we apply similarity analysis to investigate GI's efficacy in reducing peak discharge and CSO volume and the conditions under which CSOs can be eliminated for combinations of the dimensionless timescales. Section 4 illustrates how the framework can be used to manage CSO volume and frequency using the historical precipitation data in Philadelphia, PA, and Seattle, WA on a hypothetical sewershed. Finally, Section 5 and Section 6 present the discussion of results and conclusions.

2. Timescales and the proposed theoretical framework

This section outlines the proposed CSO management framework, adapted from the similarity analysis of Robinson & Sivapalan (1997). In the development of this framework, we consider a GI as an aggregation of all GI installations at one subsewershed so that the framework is scalable. This simplification allows us to focus the discussion on the timescales and the locational effects. For GI installations with the same design, the lumped GI will have storage equal to the total storage of all installations and a treated area equal to total treated area of all installations. Below, we introduce the hydrologic timescales and the intensities, and explain the CSO generating process using a conceptual example. Then, we present the proposed framework and the theoretical separation lines of CSO generating storms under that framework. A GI here is defined as a storage facility that can overflow when its storage is full. Later in Section 3 and 4, we will relax this assumption by adding other hydrological functions (i.e., infiltration and evaporation) to GI.

2.1 Hydrologic timescales and intensities

We argue that the first-order effect of GI on peak discharge and occurrence of CSOs depends on the interaction of processes encapsulated in three timescales: the storm duration, the time of concentration (i.e., the time for water to travel from the furthermost point in a watershed to the watershed outlet), and the time to fill GI storage, and two intensities: the peak discharge and the CSO discharge threshold. The first of these is the storm duration t_r, which is the temporal extent of the runoff-generating rainfall (i.e., excluding any initial period during which infiltration or interception dominates). For simplicity, we only discuss a single storm in this section and assume no within-storm variability (i.e., constant intensity i). In practice, within-storm variability is an important aspect in urban storm drainage (Chow et al., 1988), and as we shall show later, it has a significant impact on CSO occurrence and severity. As a first step, this aspect is left out of the proposed framework, and will be incorporated in future extensions of the study.

Without the presence of GI, the spatial extent of a sewershed and the pathways that concentrate local runoff toward the catchment outlet are the first-order control on the formation of a flood peak. We assume that these processes result in the emergence of a time of concentration, t_c. If the storm duration, t_r, is larger than the time of concentration, t_c, the storm intensity, i, determines the magnitude of the peak discharge Q_p (which is normalized by the area of the sewershed). When the storm duration, t_r is substantially shorter, the total discharge over the time of concentration ($\frac{it_r}{t_c}$) determines the peak, but this quantity will be lower than the maximum discharge in the previous case (we will explain this in more detail in Section 2.4). This behavior is most simply reproduced in a 'linear reservoir' model of catchment behavior, in which runoff

is proportional to storage ($Q = S/t_c$) or, equivalently, that runoff can be modeled as the convolution of the rainfall and an exponential instantaneous unit hydrograph ($Q(t) = \int_0^t i(\tau) \exp(-\frac{t-\tau}{t_c})\, d\tau$) (Chow et al., 1988). However, it can be approximately true in more complex models for an appropriate value of t_c.

Robinson and Sivapalan (1997) made similar arguments and showed that catchment response could be approximated in this form, the peak discharge depended on the interaction of t_r, t_c, and the typical time between storm events t_b. The latter helped determine the importance of antecedent wetness and carry over of effects from storm to storm. Here, we focus on a single storm with no infiltration during the precipitation (this assumption is relaxed in Section 3 and 4). In such a model, the peak discharge can be estimated as:

$$Q_p = i\left(1 - \exp\left(-\frac{t_r}{t_c}\right)\right) \tag{1}$$

The timescale t_c can be disaggregated into two elements: the travel time on the land surface, t_s, and the travel time within the stormwater drainage network, t_n. Because of the dense drainage system in urban areas, the travel time of overland flow on the impervious urban area, t_s is usually relatively small, and its typical value may not vary systematically within the catchment area. However, the sewershed travel time (t_n) scales with catchment area. Thus, for a sufficiently large catchment $t_s \ll t_n$:

$$t_c = t_s + t_n \cong t_n \tag{2}$$

This approximation allows us to analyze the sewershed response based on sewershed size but not the paths for which reliable sewer information in old cities is often not available. In the development of the theoretical framework, we assume the approximation is valid and use the network travel time (t_n) as the timescale of a sewershed instead of the time of concentration (t_c).

A third timescale is the time needed to fill GI storage during a storm, t_{GI} (called GI duration hereafter). We assume that the GI can be understood primarily as a kind of threshold storage, such that while its storage is not full, it intercepts runoff from a portion of the sewershed, and once it is full additional runoff passes through toward the outlet without substantial attenuation. When GI is present, its effect will, therefore, depend on whether it has filled. t_{GI} depends on the storage volume and the inflow to GI:

$$t_{GI} = \frac{S_{GI}}{iA_t} \tag{3}$$

where A_t is the area 'treated' by the GI; S_{GI} is the GI's storage volume; and i is the rainfall intensity. The discharge from GI is zero until t_{GI}, and equal to the rate of inflow to the GI afterward (neglecting losses in GI due to infiltration and evapotranspiration for simplicity), if the rain continues.

The occurrence of CSOs depends on whether the capacity of the combined sewer to manage stormwater has been exceeded. We simplify the CSO generating process by assuming that a CSO occurs if the peak discharge, Q_p, exceeds some threshold, Q_{CSO}. Practically, Q_{CSO} can be estimated from the weir height of the overflow device (Andrés-Doménech et al., 2010; Freni et al., 2010; Lucas & Sample, 2015) or from statistical analysis of CSOs and rainfall data (Fortier & Mailhot, 2015; Mailhot et al., 2015; Schroeder et al., 2011). Both Q_p and Q_{CSO} are normalized by the total area.

2.2 A hypothetical sewershed and a conceptual example

Consider an idealized urban sewershed (Figure 1) divided into *n* subsewersheds: S_1, S_2,…, and S_n. In each subsewershed, the runoff from impervious and pervious surfaces are generated in parallel; any GI is assumed to be installed immediately upstream of the drainage system, as Figure 1 shows.

Although this sewershed representation can include runoff generated from both impervious and pervious areas, we simplify our analysis by ignoring the effect of pervious areas, except for the GI itself (i.e., the sewershed is 100% impervious before GI was installed; or it can be viewed as two separate sewersheds: the pervious and the impervious, both draining to the same outlet). In a more general analysis, both the GI and pervious areas can have infiltration and generate runoff. However, the results are expected to be qualitatively similar because the changes in runoff and peak discharge are from the installation of GI and the impervious area draining into it.

Figure 2 shows the conceptual example where we assume an urban sewershed with three subsewersheds (dubbed Upper, Middle, and Lower), each produces (in the absence of GI) an identical unit hydrograph resulting from a uniform storm lasting for two hours (t_r =2 h) with a total rainfall of 50.8 mm (i = 25.4 mm/h). Such a storm is assumed to result in 2.5 hours of discharge from each subsewershed, and 4.5 hours of discharge at the sewershed outlet. The travel time in the drainage network from the Upper to the outlet is two hours (t_n=2 h), while for the Middle and Lower the travel times are 1 and 0 h, respectively. The resulting hydrograph (bottom-right of Figure 2) shows that the discharge exceeds the CSO threshold (Q_{CSO}) at hour 2 and continues overflowing for 1.5 hours (each bar is half an hour).

Furthermore, we assume that a typical GI unit has storage of 152.4 mm and surface area of 3.33
% of the sewershed for treating 20% area of a subsewershed. The first question we would like to answer is: does it matter where the GIs are installed and if so, where should we install the GI units? Because the GI storage can only provide one hour of stormwater reduction ($t_{GI} = \frac{152.4*3.33\%}{20\%*25.4}$ h = 1 h < t_r), its ability to reduce peak discharge and CSO will depend on whether the reduction coincides with peak discharge and CSO when it propagates to the sewershed outlet.

In this example, we install one GI unit in the Upper and another in the Lower to demonstrate how the timescales affect GI's efficacy. The bottom-right of Figure 2 shows the resulting hydrograph of the GI installed in Upper and Lower subsewersheds, where the light green boxes and dark green boxes show the flow reduction provided by the GI at Upper and Lower subsewersheds, respectively. The dotted line at the lower right of Figure 2 is the CSO threshold (Q_{CSO}) used to determine the volume of overflows. The CSO volume is calculated from the area above the threshold in the hydrograph, while any runoff below the threshold is assumed to be captured, treated, and discharged by the wastewater treatment plant. We can see that the GI in the Upper reduces both the total volume and duration of the CSO event, while the GI in the Lower has no effect.

The results above can be understood by considering the timescales involved. Without GI, the peak discharge under a constant intensity storm is controlled by the duration of the storm (t_r) for short storms ($t_n \gg t_r$), and by the network travel time (t_n) for long storms ($t_n \ll t_r$). When $t_n \gg t_r$, the peak discharge will increase as t_r increases but will be well below the maximum peak discharge (i.e., the first 2 hours in the hydrograph at the outlet in Figure 2). Therefore, it

is less likely to exceed the CSO threshold and cause overflows. On the other hand, when $t_n \ll t_r$, the discharge will reach the maximum peak discharge at t_n and continue until the storm ends. If a GI is installed at the outlet, the GI duration (t_{GI}) would need to be at least t_r to reduce peak discharge, otherwise, peak discharge cannot be reduced.

In the example above, t_r is equal to t_n. More complex dynamics arise in this case. With GI at the Lower subsewershed, the intercepted runoff would not have contributed to the peak and the overflow unless $t_{GI} > t_r$. However, the reduced runoff from the Upper subsewershed coincides with the peak discharge in the hydrograph, which substantially decreases the peak discharge and the overflow volume. Although the reduction in this example could not prevent the CSO occurrence (some CSO remains at hour 2), it is possible to prevent this CSO if the GI at the Lower were relocated to the Middle.

This linear unit hydrograph example illustrates the general idea of our analysis but does not account for the antecedent conditions, the precipitation variability, the dispersion of the flood wave and the hydrodynamics as water travels along the sewer system. More sophisticated results are presented in Section 3 and 4.

2.3 Dimensionless timescales and GI control on peak discharge

In cases like the one above, the location of GI can affect the timing of the reduction in the outlet hydrograph and thus could be critical in managing peak discharge. In other words, for storms that cause CSOs, GI's capability in controlling them could depend on its location in a sewershed and the network travel time (the time for water at the outermost inlet traveling through the sewer system to the outlet). For the case that $t_n \ll t_{GI}$, the location of GI has little effect on its performance in controlling CSO, since travel times through the network are negligible, while for the case that $t_n \gg t_{GI}$, contributions to the peak may be so dispersed in time that location in space may again be relatively unimportant. It is for the intermediate case that the location of GI becomes important because it determines which part of the hydrograph would be altered. However, the CSO reduction also depends on the storm duration, t_r.

To develop a framework for conceptualizing the role of timing in GI performance, we define two dimensionless timing ratios, T_r and T_n. T_r is the storm duration relative to GI duration, while T_n is the network travel time relative to GI duration, as shown below.

$$T_r = \frac{t_r}{t_{GI}} \text{ and } T_n = \frac{t_n}{t_{GI}} \quad (4)$$

These dimensionless ratios can be used to distinguish the cases where the GI storage, rainfall intensity and duration, and the sewershed network travel time are dominating the hydrological processes. They serve as indicators of GI's ability to control peak discharge. For example, $T_r \gg 1$ means the duration of a storm is larger than the time to fill GI's storage so that GI would be full and unable to reduce runoff volume before the storm ends, and so is not able to reduce peak discharge and CSO volume, if CSOs occur. Meanwhile, if $T_r \ll 1$, it means the storm is relative flashy, and GI can provide runoff reduction throughout the storm. $T_n \gg 1$ means that if a GI was located next to the sewershed outlet, it would be full before the runoff from the outermost point at the sewershed reaches the outlet, which is when the flow reaches its peak for sufficiently large storms. Therefore, such a GI would not be able to manage peak flow and possibly CSOs. If T_n is around 1, the location of GI and the storm duration might determine whether GI would be effective in controlling the peak discharge. On the other hand, when $T_n \ll 1$, the network travel time is relatively short so that GI can influence the peak discharge regardless of its location.

With a typical GI providing a certain depth of storage for a percentage of a subsewershed, we identify five cases corresponding to the T_r-T_n ranges shown by colored outlines with indices (a) to (e) in Figure 3.

- **(a) Trivial storm regime:** Small T_r implies small storm volume that the runoff from the treated area is completely detained by GI and T_r dominates peak discharge (outlined in gray).
- **(b) Dispersion regime:** Large T_n means strong dispersion effects so that GI-caused flow reduction would spread out widely over time and would not have a targeted influence on the peak discharge. Therefore, the dispersion dominates peak discharge (outlined in black).
- **(c) Location-relevant regime:** T_r and T_n are both close to 1 implies that the storm can be managed by GI, and the *location of GI could control its effect on peak discharge reduction*. In fact, this area is the transition zone between different mechanisms that affect the magnitude and timing of the peak discharge, and GI siting provides some flexibility to extend GI's ability in peak discharge control. Therefore, this area does not have a definitive boundary since different effects will more or less affect the resulting peak discharge. (outline in blue)
- **(d) Location-irrelevant regime:** Small T_n implies a small sewershed (small t_n) or a low-intensity storm (large t_{GI}), and $T_r \ll 1$ means that GI would not be full before peak discharge, so *the shape of the reduced peak discharge does not depend on the location of GI* (outlined in green).
- **(e) Intense storm regime:** Large T_r means that GI would be full before the storm ends. In smaller sewersheds, although GI may be able to treat some of the stormwater in the high flow period, it could not reduce sewershed discharges that contribute to the sewersheds' peak outflow, whereas in large sewersheds, the reduction would be highly dispersed and would not have significant contribution to the peak discharge control. Therefore, T_r dominates peak discharge and GI would not be effective in reducing CSOs (outlined in orange).

This timescale framework allows us to identify conditions under which GI can provide higher peak discharge reduction, which can be applied for adapting the designs or developing siting strategies. Specifically, the framework indicates that GI placement is important only in the location-relevant regime (Figure 3c). However, GI storage and the treated area would affect the values of T_r and T_n and, therefore, where a specific sewershed and storm combination falls on Figure 3. Nonetheless, this framework alone cannot tell us when a CSO can happen and how well GI can treat it. If no CSOs are present, GI's ability to manage peak discharge cannot provide any CSO reduction. Therefore, in the next section, we extend the framework to consider the threshold for triggering CSOs and introduce a dimensionless number for separating CSO-generating storms from regular storms.

2.4 A dimensionless GI threshold number and the CSO storms separation lines

As mentioned earlier, a CSO occurs when the flow exceeds the sewer system's capacity (Q_{CSO}) such that the untreated wastewater and stormwater overflows to water bodies. Based on this assumption, we approximate the critical storm intensity i^* that generates a peak discharge equal to Q_{CSO} and use it to calculate the boundary lines separating storms that produce CSOs and storms that do not (termed CSO storms and non-CSO storms, respectively). The approximation

of this critical storm intensity is divided into three cases based on the t_r/t_n value of a sewershed (i.e., t_n is a constant), as shown in Figure 4. The approximation methods for the three cases are explained as follows.

- Case A ($\frac{t_r}{t_n} \ll 1$)

  In this case, the storm duration is not long enough to reach its maximum discharge and the peak discharge can be approximated by a linear function.

  $$Q_p = Q_{CSO} = \frac{t_r}{t_n} i^* = \frac{T_r}{T_n} i^*; \text{ or } \quad i^* = \frac{t_n}{t_r} Q_{CSO} \tag{5}$$

  where i^* is the critical intensity for overflows. For a storm with a duration equal to t_r and a sewershed with network travel time t_n, a CSO would happen if the storm intensity is greater than the critical intensity i^*. Mapping this relationship to the T_r-T_n space, we can get the following inequality.

  $$T_r \geq \frac{t_r i^* A_t}{S_{GI}} = t_r \frac{\frac{t_n}{t_r} Q_{cso} A_t}{S_{GI}} = \frac{t_n Q_{cso} A_t}{S_{GI}} = GN \tag{6}$$

  For a sewershed with a given GI, t_n, Q_{CSO}, A_t, and S_{GI} are all known constants. Therefore, we can calculate the value of $\frac{t_n Q_{cso} A_t}{S_{GI}}$, called the *GI threshold number*, or *GN*. The same inequality can be derived by plugging the critical intensity, i^* in $T_n = \frac{t_n i A_t}{S_{GI}} \geq \frac{t_n \frac{t_n}{t_r} Q_{CSO} A_t}{S_{GI}} = GN * \frac{T_n}{T_r}$. By multiplying T_r/T_n on both sides, we can derive the same equation as Eq. (6).

- Case B ($\frac{t_r}{t_n} \gg 1$)

  In this case, the storm would reach its maximum discharge which is equal to the value of the storm intensity ($Q_p = i^*$). Similarly, we can derive the inequality in T_r -T_n space by setting $i^* = Q_{CSO}$:

  $$T_n \geq \frac{t_n Q_{CSO} A_t}{S_{GI}} = GN \tag{7}$$

  $$T_r \geq \frac{t_r Q_{CSO} A_t}{S_{GI}} = \frac{t_r}{t_n} \frac{t_n Q_{CSO} A_t}{S_{GI}} = \frac{T_r}{T_n} GN \tag{8}$$

  By multiplying $\frac{T_n}{T_r}$ on both sides of Eq. (8), we can get $T_n \geq GN$, which is the same inequality as Eq. (7).

- Case C ($\frac{t_r}{t_n} \cong 1$)

  As the ratio of $\frac{t_r}{t_n}$ is close to 1, the linear approximation cannot provide an adequate estimate of the peak discharge. Thus, we resort to the exponential function of a linear reservoir system (Eq. (1)) to approximate the critical storm intensity, i^*:

  $$Q_{CSO} = Q_p = i^* \left(1 - e^{-\frac{t_r}{t_n}}\right) \tag{9}$$

  By dividing both sides by i^* and replacing $\frac{t_r}{t_n}$ with $\frac{T_r}{T_n}$, we get:

  $$\frac{Q_{CSO}}{i^*} = \frac{\frac{t_n Q_{CSO} A_t}{S_{GI}}}{\frac{t_n i^* A_t}{S_{GI}}} = \frac{GN}{T_n} \leq (1 - e^{-\frac{T_r}{T_n}}) \tag{10}$$

By solving Eq. (10), we can derive the envelope curve:

$$T_n \geq GN \frac{T_r}{T_r + GN * ProductLog(\frac{T_r}{GN}\, e^{-\frac{T_r}{GN}})} \quad (11)$$

ProductLog() in Eq. (11) is the Lambert W-function, which is the inverse function of $f(w) = w\, e^w$ (Corless et al., 1996).

We call Eqs. (6) and (7) the "*CSO separation lines*" and Eq. (11) the "*CSO envelope*" which can be plotted in the T_r-T_n framework, as shown in Figure 5.

Since the intersection of the two separation lines is (*GN*, *GN*), the location of these lines depends on the value of *GN*. That is, it depends on the network travel time, CSO threshold, and the ratio of the treated area to GI storage ($\frac{A_t}{S_{GI}}$). By combining the framework for peak discharge and the CSO separation lines (and the envelope), we can infer that GI can be most efficient in treating a CSO with its storage when (*GN*, *GN*) is located in the location-irrelevant regime (d) at any location and in the location-relevant regime (c), if installed at an appropriate location. Contrarily, if (*GN*, *GN*) falls in the trivial storm regime (a), dispersion regime (b), or intense storm regime (e), the GI would not significantly contribute to CSO volume reduction in that particular situation.

3. Evaluation of GI's efficacy in reducing peak discharge and CSO under uniform storms (single storm)

This section first introduces the rainfall-runoff model that we use to evaluate more realistic hydrological responses of GI in an urban sewershed through the lens of the framework of Figure 5. Then we applied the model to the hypothetical sewershed and show the GI effectiveness in reducing peak discharge, CSO volume and occurrence with a more fine-grained examination of T_r and T_n combinations under uniform storms.

3.1 Model description

First, we introduce the rainfall-runoff model developed for our analysis, which includes the essential components of the hydrologic processes and can be easily modified to evaluate the hydrologic response of a sewershed resulting from the changes in the timing ratios (i.e., T_r and T_n). More complex rainfall-runoff models, such as EPA Stormwater Management Model (Rossman, 2015) and Soil and Water Assessment Tool, SWAT (https://swat.tamu.edu/) can also be used for our analysis, but the complexities of such models might obscure the first-order insights sought here.

The rainfall-runoff model is developed based on the mass balance equation:

$$\frac{dS}{dt} = i(t) - Q(t) - f(t) - e(t) \quad (12)$$

where *S(t)[L]* is ponded surface water storage in the catchment including the storage provided by GI, *i(t)[L/T]* is the rainfall intensity, *Q(t) [L/T]* is the discharge at the catchment outlet, *f(t)[L/T]* is the infiltration rate, and *e(t)[L/T]* is the evaporation rate. We assume that the evaporation during a storm event is negligible ($e(t) = 0$). What GI does in Eq. (12) is to increase $\frac{dS}{dt}$ by providing storage to the left-hand side of Eq. (12), as shown in Eq. (13):

$$\frac{dS}{dt} + \frac{dS_{GI}}{dt} = i(t) - Q(t) - f(t) - e(t) \quad (13)$$

This model does not consider evapotranspiration and interception provided by vegetation because the contribution of runoff reduction from evapotranspiration and interception during typical CSO events would be negligible compared to other hydrologic functions due to the high rainfall intensities and volumes involved. However, the effects of evapotranspiration and vegetation interception can be modeled using the effective precipitation in places where these effects are not negligible.

3.1.1 Infiltration

We assume that the portion of the sewershed draining into the GI is completely covered impervious surface and the installation of GI converts just its site from the impervious surface to pervious. Therefore, infiltration only happens on the footprint of the GI itself. The infiltration process is modeled by the Green-Ampt equation (Chow et al., 1988), which is solved after the time of ponding.

$$F(t) = K_s t + \psi_s \theta_d \, ln\left(1 + \frac{F(t)}{\Psi_s \theta_d}\right) \tag{14}$$

where $F[L]$ is the cumulative infiltration, $K_s[L]$ is the saturated hydraulic conductivity, $\Psi_s[L]$ is the capillary suction head, and θ_d[-] is the water deficit in soil. The infiltration rate $f(t)$ can be calculated from *F(t)* by Eq. (15).

$$f(t) = K_s\left(\frac{\Psi_s \theta_d}{F(t)} + 1\right) \tag{15}$$

Before ponding, the infiltration rate *f(t)* is assumed equal to the rainfall intensity and the time for the soil to recover to dry conditions is assumed 24 hours after the storm stops and ponding water is completely drained.

3.1.2 Overland flow

Overland flow is modeled by Manning's equation as shown in Eqs. (16) and (17).

$$Q(t) = \frac{1}{n} A S_f^{1/2} R_h^{2/3} \tag{16}$$

where $Q(t)$ $[L^3/s]$ is the overland flow rate, n $[T/L^{\frac{1}{3}}]$ is the Manning's coefficient, $A[L^2]$ is the flow cross-section area, S_f [-] is the slope of the hydraulic grade line which can be approximated by the slope of channel bed (assuming kinematic wave), and $R_h[L]$ is the hydraulic radius. Let w $[L]$ denote the effective width of the overland flow and d denote the ponding depth. Given $A = dw$ and $R_h = A/P$ where P is the wetted perimeter ($w \gg d, P = 2d + w \cong w$), we can rewrite Eq. (17) using w and d.

$$Q(t) = \frac{1}{n} w S_f^{1/2} d^{5/3} \tag{17}$$

3.1.3 Flow routing

We chose the Muskingum method (Cunge, 1969) to model flow routing for its simplicity. Eq. (18) is the general expression of the Muskingum method.

$$dS/dt = K[xI + (1 - x)O] \tag{18}$$

where *I* is the inflow rate, *O* is the outflow rate, and *K* and *x* are the storage parameters. The value of *K* can be viewed as the travel time of the wave travel through the catchment. Meanwhile, *x* is a weight coefficient of the contribution from inflow to the storage that controls the dispersion of a flood wave in the channel with a typical value in the range of (0, 0.5) (Strupczewski & Kundzewicz, 1980).

3.1.4 Evaporation

We assumed that the evaporation rate *e(t)* is negligible during a storm event and, after the storm, *e(t)* is 2.4 mm/day. The evaporation rate after storm (range from 1.3 mm/day to 3.8 mm/day) is chosen based on the daily average evaporation data in Washington (Western Regional Climate Center, 2020) and Pennsylvania (Northeast Regional Climate Center, 2020) . This only controls the volume of ponded storage and not the antecedent soil water deficit θ_d. The influence of temperature and vegetation on evaporation are not included in this model for simplicity.

3.2 Hydrological response of a hypothetical sewershed with GI at various locations under uniform storms

This numerical analysis is designed to show how the hydrograph depends upon the proposed dimensionless timing ratios, T_r and T_n, for hypothetical urban sewersheds (100% impervious) with three subsewersheds (Upper, Middle, and Lower), under uniform storms. The storm intensity, i, is constant for all simulations and the storm duration, t_r changes with the specified T_r to represent storms with various durations. t_{GI} is also a constant so that the variations in T_r and T_n depend only on the values of t_r and t_n. t_n is estimated based on the storage parameter of the Muskingum method, K, for each channel segment; therefore, a sewershed with n subsewersheds can be approximated by $t_n = \sum_{i=1}^{n} K_i$. Moreover, the shape of the sewershed is assumed unchanged, such that the increases in t_n correspond with the increase in the square root of the total sewershed area. To facilitate the comparison of model results, the discharge is normalized by the sewershed area. This practice applies to all the numerical analyses of this paper.

The rainfall-runoff model described in the previous section was applied to assess the sewershed response with GI installed at the Lower and Upper subsewershed, respectively. We assume that a uniform storm has an intensity of 12.7 mm/h (0.5 in/h) and duration of t_r hours. The length of the overland flow is set to a small number (30.5 m throughout this paper; t_s is less than 10 minutes) so that we can approximate t_c with t_n. In addition, we assume that 30% of the total area ($A_t = 0.3$) drains into the GI with a surface area of GI itself equal to 5% of the total area, and a storage depth of 152.4 mm under the GI surface area (effective GI storage depth: $152.4 \text{ mm} * 0.05/0.3 = 25.4$ mm = 1 inch; GI storage depth normalized by sewershed area: $S_{GI} = 152.4 \text{ mm} * 0.05 = 7.62$ mm) so that t_{GI} is equal to 2 hours.

As we can see, the hydrographs in Figure 6 are consistent with our expectation although the magnitude of the competing effects would depend on the T_r and T_n values. For example, we can see that GI location can result in different levels of peak discharge reduction in the case of T_r and T_n equal to 0.5 (bottom row, Figure 6a,), while it is less obvious in the case of T_r and T_n equal to 3 (right column, Figure 6b) since the dispersion dominates the process.

For small storms (Figure 6a), we can see that the normalized peak discharge and discharge reduction decease as T_n increases due to the increased dispersion of the flood peak along the channel, while for large sewersheds (Figure 6b), the dispersion would dominate the sewershed response by lowering the normalized peak discharge and attenuating the reduction provided by GI. Around $T_r \approx 1$ (Figure 6c and d), GI can fully utilize its storage to contain stormwater at the time the storm ends. If GI is located at Upper, the discharge reduction can be delayed as much as t_n, which means that we could manage peak discharge by carefully choosing the location of GI. However, if $t_n + t_{GI} \ll t_r$ (or equivalently $T_n + 1 \ll T_r$), it is impossible to reduce peak discharge (Figure 6e), since, in this case, GI storage will be full before the peak occurs.

In general, GI location does not have much influence on the discharge reduction for the cases on the bottom row in Figure 6 ($T_n = 0.5$). However, for cases related to the middle and upper rows (Figure 6b and c), the timing of the discharge reduction would shift to the right when relocating GI from the Lower to Upper subsewersheds. The hydrographs help us understand how GI siting can affect peak discharge reduction but what combinations of T_r and T_n are more effective in providing CSO reduction is not apparent due to the dispersion.

To further investigate how urban systems react to the values of the timescales and the GI location, we simulate combinations of T_r and $T_n$with a finer resolution to show the overall view of the system response and the effect of GI location on peak discharge and CSO in the following section.

3.3 GI's efficacy of reducing peak discharge and CSOs for T_r-$T_n$combinations

This section presents two analyses in the ideal world (uniform storms). The first analysis focuses on applying the framework to identify the situations in which GI can be more effective in reducing peak discharge and CSO volume, whereas the second analysis investigates GI's effectiveness in treating CSOs frequency (i.e., to reduce CSO volume to zero).

3.3.1 How much peak discharge and CSO reduction can GI achieve?

In this section, we use the simulation model to investigate GI's effectiveness under various T_r-T_n combinations. More specifically, we vary t_r and t_n to test the GI siting effects in sewersheds of different sizes under uniform storms with different storm duration, while t_{GI} is fixed as a constant. The storm intensity is set to 12.7 mm/h. Because the dispersion in large sewersheds (surface area ≥2,000 ha or t_n ≥3 h) will lower the peak flow to below the CSO threshold and generate no CSOs, we compensate the dispersion effects by adjusting the CSO threshold as t_n increases so that the uniform storms can still generate CSOs. The adjustment is done by making $t_n Q_{cso}$ = 22.86 mm (e.g., Q_{CSO} equals to 7.62 mm/h, if t_n is 3 hours and Q_{CSO} equals to 22.86 mm/h, if t_n is 1 hour). The resulting GI threshold number is, therefore, 0.9. (GN = $\frac{t_n Q_{CSO} A_t}{S_{GI}} = \frac{22.62*0.15}{3.81} \cong 0.9$). This adjustment assumes similarity in sewer systems. That is, the travel time (t_n) and the CSO threshold (actual and unnormalized value; Q_{CSO} is the threshold normalized by the sewershed area) are proportional to the square root of the sewershed area so that $t_n Q_{cso}$ remains a constant.

In addition, the number of subsewersheds is increased to five, the storage of GI (normalized by the sewershed area) is set to 3.81 mm (storage depth: 152.4 mm; GI surface area: 2.5% of the sewershed area), and the treated area (A_t) is reduced to 15% of the total area (therefore, $t_{GI} = \frac{152.4*2.5\%}{12.7*15\%} = 2$ hours), so that the simulations would be more sensitive to the location of GI. The subsewersheds, from upstream to downstream denoted by S_1, S_2, S_3, S_4, and S_5, are assumed 100% impervious and identical. The resulting peak discharge is normalized by storm intensity and plotted in T_r-T_n space, as shown in Figure 7, whereas the resulting CSO reductions are normalized by total storm volume and plotted in Figure 8.

The colored outlines imposed on the raster maps in Figure 7 represent the peak discharge regimes identified in Figure 3. To start with, Figure 7a shows the normalized peak discharge without GI, where we can see that, when $T_r < T_n$, the peak discharge decreases as T_n increases, capturing the stronger dispersion effects in large sewersheds. Figure 7b, c, d, e, and f show the normalized peak discharge reduction by locating GI in each subsewershed from upstream to downstream, respectively. We can see that the maximum peak reduction is about 15.1% of the

maximum peak discharge regardless of the GI location (the extra 0.1% is mainly from infiltration), so that the higher reduction area shifts to the right as T_n increases, and that the shift increases as GI moving upstream. The shift of the high reduction area is resulted from the combination of the dispersion and the network travel time of the reduction, which is stronger in a larger sewershed and when GI is located upstream. Furthermore, the colored outlines in the subfigures highlight the regions where different mechanisms dominate the peak reduction in Figure 7, as explained in Section 2.3

The location-irrelevant regime (the green box) in each map is located at $T_r \in (0.5, 1.3)$ and $T_n \in (0.1, 0.5)$ for the following reasons:

- When $T_r \in (0.5, 1.3)$, GI storage is actively filling during the high-discharge period, including the high-flow recession period, so it could provide greater peak reduction. The upper bound of T_r will be higher with stronger effects of infiltration, and depression storage.
- Small T_n means the network does not disperse the discharge reduction across the hydrograph. If GI could reduce peak discharge, it will do so regardless of where it is in the network.

In addition, the location-relevant regime (the blue dashed outline) in each map highlights the region that GI is reasonably effective but sensitive to GI location. Just focusing on the location-relevant regimes in Figure 7b, c, d, e, and f, we can see that having GI at S_3 or S_4 can provide a higher reduction in the range but what location of GI could provide the highest peak discharge reduction would depend on the T_r and T_n combinations.

GI's ability to reduce peak discharge does not equal its ability to reduce CSO volume. In Figure 8, we turn to the analysis of CSO volumes where the results are normalized by total storm volume. Figure 8a shows that the normalized CSO volume increases along the diagonal direction. The theoretical separation lines and the envelope curve outline the region in the T_r-T_n space that generates CSOs. GI is effective in reducing CSO volume for the T_r-T_n combinations tested in this analysis; however, the reduction depends on the location of GI and the specific T_r-T_n combination. Judging from the dark area, siting GI in the Upper and Middle subsewersheds (Figure 8b and d) works better than siting GI in Lower subsewershed (Figure 8f) for most T_r-T_n combinations. This is because GI at Lower uses most of its storage to treat stormwater before CSO starts, whereas the runoff reduction provided siting GI at Middle and Upper is more likely to coincide with CSO when it propagates to the sewershed outlet.

To summarize, for small sewersheds and mild and intermediate storms (location-irrelevant regime, Figure 3d), GI's capacity to reduce peak discharge and CSO volume does not depend on its location, while for medium sewersheds (location-relevant regime, Figure 3c), locating GI at S_2, S_3 or S_4 can retain more stormwater that would otherwise contribute to CSOs.

This finding implies a tradeoff between managing CSO frequency and volume. For minor CSO events, peak discharge reductions can eliminate the CSOs and therefore reduce the *frequency* of CSOs. However, a strategy emphasizing reduction of CSO *volumes* (e.g., by siting in S_2) may not be as useful for managing CSO frequency (for which S_3 and S_4 are more effective). To further investigate how GI can eliminate CSOs, we simulate the same T_r and T_n in the same sewershed (t_n is fixed) while changing the storm intensity and duration to see the effects.

3.3.2 What CSOs can be fully treated by GI in a sewershed?

The presence of CSOs often results in disturbance of the beneficial uses of water (e.g., beach closings) for the deteriorated water quality the CSOs caused. If the purpose of stormwater

management is to prevent the disturbance of beneficial uses, the control efforts should be focused on eliminating CSOs. In this simulation, the network travel time is set to 3 hours to represent an urban sewershed of a small size city (area approximately 2,000 ha), and CSO threshold is set to 7.62 mm/h so that the GN is also 0.9. We test the same T_r-T_n combinations but the variables have changed to storm intensity and duration (i and t_r) so each T_r-T_n combination represents a uniform storm.

In Figure 9, we can see that the 100%-reduction area (black area) follows the CSO separation lines and the envelope curve, however, the shape of the area changes with the location of GI. When siting GI in the Upper, it is most effective in eliminating CSOs for storms with peak discharge slightly higher than CSO threshold and longer duration (Figure 9b), whereas when siting GI in the Middle or the Lower, GI is more effective in eliminating CSO with T_r slightly higher than 1. The 100%-reduction area can be expanded with an increase of the treated area. Moreover, by comparing the Figure 8 and 9, we can see that the regions where GI can eliminate CSOs yield only limited CSO volume reduction which suggests that to manage CSO frequency with GI requires a different design and placement strategy.

The above analysis focuses on the impact of GI location, sewershed and storm characteristics on CSO volume and frequency reduction under uniform storms. However, the goal of implementing GI is to reduce long-term stormwater pollution over the full range of precipitation events and to enhance water quality in water bodies. As the nature of precipitation is highly variable and intermittent between and within storms, the GI efficacy may also vary with the storm patterns. Stormwater managers are likely to be most interested in GI's long-term efficacy given the climate conditions on the sewersheds they managed. Therefore, in Section 4, we apply historical precipitation data in two cities as examples to assess GI long-term efficacy in managing CSO volume and frequency under different climate conditions as a function of the GI location.

4. Evaluation of GI performance with long-term precipitation records (multiple storms)

In this section, we applied the rainfall-runoff model with 34 years of observed precipitation data on the hypothetical sewershed with five subsewersheds, labeled from upstream to downstream as S_1, S_2, S_3, S_4, and S_5, respectively. The precipitation data are assumed warm weather rainfall since most CSOs happen during rainstorms. In addition, we assume that the network travel time (t_n) is 3 hours, 20% of the total area draining into the GI (i.e., $A_t = 20\%$), and the GI storage depth normalized by the sewershed area (GI storage depth: 152.4 mm; GI surface area: 3.33% of the sewershed area) is 5.07 mm.

We chose Philadelphia, PA and Seattle, WA for this analysis because of their wet climate and distinct precipitation patterns. Philadelphia has more intense and short-duration thunderstorms while Seattle tends towards long-lasting drizzles. The hourly precipitation data applied in this analysis were recorded at Philadelphia International Airport (PA) and Seattle Tacoma International Airport (WA) from 1980 to 2013, and retrieved from NOAA's CDO website (www.ncdc.noaa.gov/cdo-web/).

The precipitation records are divided into storm events. Storm events were assumed to be periods of precipitation separated by a break of at least 2 hours. Periods of no precipitation fewer than 2 hours were considered part of a larger storm. Figure 10 shows histograms of the storm characteristics (duration, mean intensity, total volume, and maximum intensity) in Seattle and Philadelphia, where we can see that the average annual precipitation in Philadelphia (1,059 mm/yr) and Seattle (945 mm/yr) are similar. However, Seattle has mostly long-duration storms with a low average and maximum intensity, while Philadelphia has more high-intensity low

duration storms. This operation only applies to Figure 10. The rest of the analyses in this section do not exclude any storms.

4.1 CSO storm statistics

We chose Q_{CSO} to be 5.08 mm/h and 2.54 mm/h for Philadelphia and Seattle, respectively, so that the resulting number of annual CSO events are at the same level (Philadelphia: 8.3 CSOs/yr; Seattle: 8.6 CSOs/yr). The simulated CSO frequency of the stormwater outlets in Philadelphia and Seattle in 2018 ranges from 2 to 85 and 0 to 45 per year, respectively (Philadelphia Water Department, 2018; Seattle Public Utilities, 2019). We chose a threshold that yields an average CSO frequency of about 8 to 9 per year for the two sewersheds so that we can compare how the precipitation pattern affects CSO generation and GI. This criterion to select the threshold value is mainly for illustration. More precise CSO threshold estimates could come from sewer system capacity and statistical analysis with precipitation and CSO data (Fortier & Mailhot, 2015; Freni et al., 2010; Sebti et al., 2016), but that is beyond the scope of this study.

Figure 11 shows the reductions in average annual CSO volume and occurrence both with GI for each subsewershed in the hypothetical sewersheds in the two cities. The error bars show the standard errors of the average annual CSO volume and occurrence reductions based on the 34-year data. The results show that siting GI in the Middle (S_3) could provide higher CSO volume reduction in Philadelphia, but it is less true for Seattle where CSO volume reduction is only slightly higher at S_3 than S_2 and S_4. Interestingly, for CSO occurrence reduction, the highest average reduction is to site GI at S_4 instead of S_3 in both cities, though the difference in reduction is smaller than the standard error (the error bar).

Table 1 shows the relative frequency at which subsewershed provides the most and the least reductions among the five subsewersheds in the two cities. We can see that locating GI at S_3 (Middle) is the best strategy for both Philadelphia and Seattle for about 60% or more of the years, while locating GI at S_2 and S_4 can be a good alternative occasionally. Siting GI at S_5 tends to be less effective for most years (25 years for Philadelphia and 27 years for Seattle). S_1 is the second-worst location - the worst for Philadelphia for 9 years and the worst for Seattle for 7 years. The results of Figure 11 and Table 1 also suggest that the GI siting strategy would be different for CSO volume and frequency, as discussed in Section 3.3.2.

4.2 Evaluation of GI's efficacy in CSO frequency reduction with historical storms

We now analyze the series of storms and their runoffs for the two cities using the theoretical separation lines and the envelope curve. We use the term *treatable storms* to designate CSO storms that can be eliminated by siting GI at any of the five subsewersheds; meanwhile, *non-CSOs* are storms that do not cause CSOs and *persisting storms* are those storms that cannot be eliminated by GI at any location. Treatable storms are further divided into two categories:

- *Loc-relevant storms*: the CSO is eliminated by GI only when siting at an appropriate location
- *Loc-irrelevant storms*: the CSO is eliminated by GI siting at any location

Figure 12 shows the storms in Philadelphia and Seattle from 1980 to 2013 on a hypothetical sewershed with t_n equal to 3 hours, the CSO separation lines and the envelope curve in Log(Tr)-Log(Tn) space, where the storms are colored into the four categories: non-CSO storms (in hollow circles), loc-irrelevant CSOs (in blue left-pointing triangles), loc-relevant CSOs (in red stars), and the persisting CSOs (in black right-pointing triangles). Traversing the diagram from lower-left to upper-right, we can see a transition from non-CSOs, loc-relevant CSOs, loc-relevant CSOs, to the

persisting CSOs, although the boundaries between categories are fuzzy. Since moving to the upper-right direction in Figure 12 means an increase in mean storm intensity, the transition is as expected.

Interestingly, the CSO separation lines and the envelope curve in Figure 12 contain only a fraction of the CSO storms. The separation line defined by $T_r = GN$ works well on this data set, but $T_n = GN$ and the CSO envelope curve do not align with the CSO storms. It could be for the following reasons:

- Prolonged storms with a lower mean storm intensity could have spikes of intense rainfall due to the within storm variability, which would generate CSOs.
- Prolonged storms may have mild rainfall that fills GI's storage at the beginning of the storm so that GI loses its capacity to capture CSOs when the high flow arrives.

Here we apply two adjustments for the separation lines and the envelope to better capture the CSOs: change the critical storm intensity from mean intensity to 90%-quantile intensity (e.g., the second-highest intensity for a 10-hour storm and the highest intensity for storms ending in 9 hours), and an adjustment factor to shift the separation lines and the envelope downward. We modified Eqs. 7 and 11 by multiplying a fraction, a, on the right-hand side, as Eqs. 19 and 20 show, to shift the separation lines and the envelope curve.

$$T_n > a * GN \tag{19}$$

$$T_n > a * GN \frac{T_r}{T_r + GN * ProductLog(\frac{T_r}{GN} e^{-\frac{T_r}{GN}})} \tag{20}$$

Figure 13 shows the results of the adjustment. All the subplots use the 90%-quantile intensity as the critical storm intensity and only the subplots on the bottom row apply the adjustment factor of 0.6 and 0.8 to Philadelphia and Seattle, respectively. We believe that the 90%-quantile intensity better characterizes CSO storms since peak discharge is likely to coincide with the peak or relatively high intensity. The fractions of 0.6 and 0.8 are selected by visual inspection, which represents the errors from our simplifications. Although the fractions a = 0.6 and a = 0.8 work well for the historical storms in Philadelphia and Seattle, this parameterization must depend on the climate patterns and the sewershed characteristics as well as the model assumptions. A more general and theory-based method to approximate and adjust the boundary lines is the subject of future research.

4.3 Evaluation of GI's efficacy in CSO volume reduction with historical storms

In this section, we apply the framework to identify the regions in which GI could be more effective in reducing CSO volume. The results are as shown in Figure 14.

If a CSO storm is fully treated by GI (no CSO after treatment), the colored circle (either blue, yellow or red) would completely overlap with the hollow circle, such as most of the blue circles on the right column (Seattle) in Figure 14. For medium and large CSO storms, although more CSO volume is captured, it could also have a large portion of untreated CSO, as the red circles and the hollow circles in the intense storm regime (e) in Figure 14 show. Comparing the second row in Figure 14 to the first row and the third row, we can see that relocating GI from S_3 to either S_1 or S_5 in Philadelphia causes in decreasing the GI performance in many CSO storms (reduction circles change color from red to yellow or from yellow to blue). In contrast, the effect of moving the GI location in Seattle results in only a moderate change in the CSO reductions. The placement of the peak discharge regimes is located according to the lines: $T_n = 1$ and $T_r = 1$ but can be adjusted based on the sewershed characteristics and the climate conditions. The results are consistent with the peak discharge regimes as many CSOs show locational

effects that are found in the location-relevant regime (c) and many CSOs showing little locational effect are found in the-location irrelevant regime (d) (many storms in Seattle, but only a few in Philadelphia). However, we also observe that many CSOs fall into the wrong categories where the framework predicts a locational effect, but the simulation results say otherwise and vice versa. The unexpected results are due to the within storm variability, antecedent conditions, and the storm partition method, which were neglected in this study. These effects are important and will need to be addressed in future studies.

Also, GI's capability to reduce peak discharge does not equal its capability to reduce CSO volume. In fact, many of the CSO storm volumes in the intense storm regime (e) can be reduced by an amount equivalent to 40% or more of the storage in the GI installations (red circles) and could significantly contribute to annual CSO volume reductions. However, the reductions in these CSOs will not have significant impacts on water quality for the small fractions they are to the total CSO volumes.

5. Discussion

Our proposed framework is based on the concept of a linear reservoir system, the dimensionless timescales (T_r and T_n), and a dimensionless number (GN). The main goal of this framework is to generate improved understanding of the interactions between GI, the sewersheds, and the climate in controlling peak discharge, CSO volume and CSO frequency.

The theoretical framework implies that, for GI to be effective in controlling CSO volume, GI placement and designs should be based on the local precipitation and the sewersheds' overflow thresholds. The GN value and the CSO separation lines can serve as indicators of whether a GI has sufficient storage to treat the CSOs. For example, if the GN value in a sewershed is greater than 1, the stormwater manager may consider increasing GI storage or reducing the treated area to ensure GI functioning during the CSO period. Doing so, the GN separation lines and the CSO storms in the T_r-T_n space will shift towards the bottom-left, which brings the CSO storms to the regimes where GI can be most effective (location-relevant and location-irrelevant regimes, Figure 3c and d). By adjusting GI storage or reducing the treated area, the CSO storms and the CSO separation lines will move along the diagonal direction in the T_r-T_n space, and therefore the framework can be used to guide GI design. The ratio of the GI storage to the treated area can be viewed as the target precipitation volume (in *mm*). The framework is only sensitive to the target volume and is not sensitive to the storage depth or the treated area as long as the ratio remains unchanged. Moreover, the installation of green or gray infrastructure can be viewed as a fortification of the existing stormwater infrastructure. For example, Figure 13 shows that adding a GI to the hypothetical sewershed can remove some CSOs which can be interpreted as an increase in the CSO threshold (Q_{CSO}) and, therefore, an increase in the GN value. This effect is also observed in the literature (Schroeder et al., 2011).

Depending on where the targeting storms are in the T_r-T_n space, a stormwater manager can decide whether a GI siting strategy is needed. This also implies that the storage volume of GI needed for different sewersheds in a city should be based on the sewersheds' CSO thresholds, as they will affect the GN value and what storms cause CSOs. Current practices in US cities are to set the storage for treating a target storm volume, for example, 25.4 mm to 38.1 mm (1 inch to 1.5 inches) in Philadelphia. We believe that the theoretical framework can help improve current practices by incorporating the CSO threshold in GI storage design.

Although we did not have the field data to validate how the changes in GI design and siting can affect its efficacy, we do find the framework consistent with findings in the literature. For example, the linear relationship between peak discharge reduction and GI treated area found in

Palla & Gnecco (2015) and Bell et al. (2016) can be explained by the framework – small sewersheds and light rainfalls would likely result in low T_r and T_n values that fall in the trivial storm regime (Figure 3a). Furthermore, we show that the location of GI can affect GI's ability to reduce both peak discharges and CSOs, especially for sizable sewersheds. The locational effects are also reported in the literature, although the observations may be complicated by local topography and the GI designs (Ercolani et al., 2018; Fry & Maxwell, 2017). On the other hand, if the information on GI location is not considered, low correlations between peak discharge reduction and GI-related metrics are also expected, as Bell et al. (2016) have shown. The validation of this framework with field survey data will be our immediate future direction.

A major limitation of this framework comes from the precipitation variability and heterogeneity of the sewershed landscape. As Figure 6 and 7 show, the framework is capable of identifying the area in the T_r-T_n space where GI is effective in reducing the peak discharge and the CSO volume in the ideal situation. However, when we applied the historical precipitation data from Philadelphia and Seattle, we see that the results are affected by the imperfect conditions, such as within-storm variability and antecedent wetness. This effect may be amplified by applications in real sewersheds where pervious and impervious areas are interwoven, and all kinds of GIs are scattered. Future work can address the direct effects of within-storm patterns and antecedent conditions.

Another limitation is that this framework only works with one GI at one location. With multiple GIs at multiple locations, it is unclear whether the GIs could eliminate a CSO and how the CSO volume reduction from each GI aggregates. For example, if a CSO storm cannot be eliminated by combinations of GIs and all the GIs can function throughout the storm event ($T_r \geq 1$), we can combine the CSO volume reduction. However, if a GI could fully treat a CSO, adding another GI would not improve the reduction in CSO volume nor in CSO frequency. Or, if multiple GIs combined could eliminate a CSO but neither could fully treat that CSO by itself, we would expect to see some GIs contribute less to CSO volume reduction than when they stand alone. The interactions between GIs are the effects of the higher order terms that are not included in this framework. However, this timescale framework can serve as a foundation for studies to investigate the higher order effects systematically.

Finally, detailed hydrologic and hydraulic simulations are needed to facilitate the use of this framework in GI planning. As Figure 13 and 14 show, the framework would require adjustments in applications with variable precipitation. The adjustments should be made based on hydrological analyses. In addition, there are several assumptions made in our analysis that can have a substantial impact on the assessment of the CSO metrics (volume and frequency) and the GI's ability to control CSOs. These factors include sewer baseflow, leaking pipes (groundwater infiltration and exfiltration into sewer systems), soil permeability, groundwater level, evapotranspiration, and other GI types (e.g., detention GI with outlet control and stormwater disconnection) (Lim & Welty, 2018; Lucas & Sample, 2015; Pennino et al., 2016). The framework can provide insights into the first-order controls of CSOs but to address these complications, detailed models, (e.g., SWMM and SWAT) are needed.

6. Conclusions

Green Infrastructure (GI) has gained increasing popularity as a greener solution for treating urban stormwater pollution. However, holistic methods for systematically evaluating the GI's efficacy have not yet appeared in the literature. This paper attempts to fill this gap by proposing a theoretical framework using which we showed that the GI's effectiveness in managing peak

discharge and CSOs depends on two dimensionless timescales, T_r and T_n (respectively, the duration of a storm and the network travel time of a sewershed, both normalized by the time to fill GI storage), and a dimensionless number, GN.

The theoretical framework provides an alternative to full detailed, physically-based modeling for GI efficacy assessment, as the dimensionless numbers (T_r, T_n and *GN*) can be estimated from precipitation data, sewershed area, and GI design parameters. In contrast, traditional methods require data for detailed parameterization that are often unavailable (Fry & Maxwell, 2017; Kong et al., 2017).

The results of numerical experiments demonstrate that GI can typically mitigate peak discharge and CSO volume for storms in a narrow band in T_n - T_r space, as identified in the theoretical framework. Within that band, the efficacy of GI may depend on the location of GI within the sewershed if network routing substantially affects the timing and magnitude of flood peaks. This information can help stormwater managers develop GI design guidelines and stormwater control plans for the sewersheds managed.

In addition, we applied the proposed framework to examine the effectiveness of GI using historical precipitation data from two major US cities: Philadelphia, PA and Seattle, WA. The results suggest that GI location is an important control on catchment-scale GI efficacy in Philadelphia, but less so in Seattle due to the difference in their precipitation patterns. To apply the theoretical separation lines and the envelope for CSO frequency control, we show that two adjustments are needed to account for the within-storm variability: the critical intensity (e.g., 90%-quantile intensity) and an adjustment factor. The adjustment can be viewed as a correction factor to characterize the effects of real storms as compared to uniform storms, and the adjustment will depend on the precipitation pattern in the sewersheds of interest. Similarly, when applying the framework to a real urban sewershed, we expect that an adjustment for the network travel time, t_n, will be needed. This is another future research direction we would like to take on.

We have shown that the theoretical framework can help identify the mechanisms that govern GI's ability to reduce peak discharge, CSO volume, and CSO frequency. Therefore, this framework can assist GI planning by providing insights on locational, and CSO volume and frequency tradeoffs. The framework is not, however, a substitute for detailed design procedures, which must consider local climate, sewershed characteristics, and engineering and policy concerns.

Besides the future directions discussed above, our immediate future work on improving this theoretical framework includes the development of methods and tools for characterizing within-storm intensity patterns, network travel time, adjustment of the CSO separation lines and the CSO envelope, optimizing the design and siting of GI for CSO control, and applications in real sewersheds. Another future direction is to incorporate groundwater into the framework, guided by the work of Lim & Welty (2017, 2018) who pointed out that the locational effects can be amplified by the presence of substantial subsurface stormflow in the rainfall-runoff response in the urban watershed.

Acknowledgment

This publication was made possible by USEPA [Grant Numbers 83555501]. Its contents are solely the responsibility of the grantee and do not necessarily represent the official views of the USEPA. Further, USEPA does not endorse the purchase of any commercial products or services mentioned in the publication. We thank the editor and the reviewers for the comments to improve this manuscript and D. Wilusz for the help in storm pattern analysis. No new data

is presented. The historical hourly precipitation data is available on NOAA CDO website: https://www.ncdc.noaa.gov/cdo-web/.

Reference

Andrés-Doménech, I., Múnera, J. C., Francés, F., & Marco, J. B. (2010). Coupling urban event-based and catchment continuous modelling for combined sewer overflow river impact assessment. *Hydrology and Earth System Sciences*, *14*(10), 2057–2072. https://doi.org/10.5194/hess-14-2057-2010

Barbosa, A. E., Fernandes, J. N., & David, L. M. (2012). Key issues for sustainable urban stormwater management. *Water Research*, *46*(20), 6787–6798. https://doi.org/10.1016/j.watres.2012.05.029

Bell, C. D., McMillan, S. K., Clinton, S. M., & Jefferson, A. J. (2016). Hydrologic response to stormwater control measures in urban watersheds. *Journal of Hydrology*, *541*, 1488–1500. https://doi.org/10.1016/j.jhydrol.2016.08.049

Casal-Campos, A., Fu, G., Butler, D., & Moore, A. (2015). An integrated environmental assessment of green and gray infrastructure strategies for robust decision making. *Environmental Science and Technology*, *49*(14), 8307–8314. https://doi.org/10.1021/es506144f

Chocat, B., Ashley, R., Marsalek, J., Matos, M. R., Rauch, W., Schilling, W., & Urbonas, B. (2007). Toward the sustainable management of urban storm-water. *Indoor and Built Environment*, *16*(3), 273–285. https://doi.org/10.1177/1420326X07078854

Chow, V. Te, Maidment, D. R., & Mays, L. W. (1988). *Applied Hydrology*. New York: McGraw-Hill.

Corless, R. M., Gonnet, G. H., Hare, D. E. G., Jeffrey, D. J., & Knuth, D. E. (1996). On the Lambert W function. *Advances in Computational Mathematics*, *5*(1), 329–359. https://doi.org/10.1007/BF02124750

Cunge, J. A. (1969). On the subject of a flood propagation computation method (musklngum method). *Journal of Hydraulic Research*, *7*(2), 205–230. https://doi.org/10.1080/00221686909500264

Ercolani, G., Chiaradia, E. A., Gandolfi, C., Castelli, F., & Masseroni, D. (2018). Evaluating performances of green roofs for stormwater runoff mitigation in a high flood risk urban catchment. *Journal of Hydrology*, *566*(September), 830–845. https://doi.org/10.1016/j.jhydrol.2018.09.050

Fortier, C., & Mailhot, A. (2015). Climate change impact on combined sewer overflows. *Journal of Water Resources Planning and Management*, *141*(5), 04014073. https://doi.org/10.1061/(ASCE)WR.1943-5452.0000468

Freni, G., Mannina, G., & Viviani, G. (2010). Urban storm-water quality management: Centralized versus source control. *Journal of Water Resources Planning and Management*, *136*(2), 268–278. https://doi.org/10.1061/(ASCE)0733-9496(2010)136:2(268)

Fry, T. J., & Maxwell, R. M. (2017). Evaluation of distributed BMPs in an urban watershed-High resolution modeling for stormwater management. *Hydrological Processes*, *31*(15), 2700–2712. https://doi.org/10.1002/hyp.11177

Fu, X., Goddard, H., Wang, X., & Hopton, M. E. (2019). Development of a scenario-based stormwater management planning support system for reducing combined sewer overflows (CSOs). *Journal of Environmental Management*, *236*(August 2018), 571–580. https://doi.org/10.1016/j.jenvman.2018.12.089

Golden, H. E., & Hoghooghi, N. (2018). Green infrastructure and its catchment-scale effects: an emerging science. *Wiley Interdisciplinary Reviews: Water*, *5*(1), e1254. https://doi.org/10.1002/wat2.1254

Jarden, K. M., Jefferson, A. J., & Grieser, J. M. (2016). Assessing the effects of catchment-scale urban green infrastructure retrofits on hydrograph characteristics. *Hydrological Processes*, *30*(10), 1536–1550. https://doi.org/10.1002/hyp.10736

Jean, M. È., Duchesne, S., Pelletier, G., & Pleau, M. (2018). Selection of rainfall information as input data for the design of combined sewer overflow solutions. *Journal of Hydrology*, *565*(August), 559–569. https://doi.org/10.1016/j.jhydrol.2018.08.064

Jefferson, A. J., Bhaskar, A. S., Hopkins, K. G., Fanelli, R., Avellaneda, P. M., & McMillan, S. K. (2017). Stormwater management network effectiveness and implications for urban watershed function: A critical review. *Hydrological Processes*, *31*(23), 4056–4080. https://doi.org/10.1002/hyp.11347

Jothityangkoon, C., & Sivapalan, M. (2009). Framework for exploration of climatic and landscape controls on catchment water balance, with emphasis on inter-annual variability. *Journal of Hydrology*, *371*(1–4), 154–168. https://doi.org/10.1016/j.jhydrol.2009.03.030

Kong, F., Ban, Y., Yin, H., James, P., & Dronova, I. (2017). Modeling stormwater management at the city district level in response to changes in land use and low impact development. *Environmental Modelling and Software*, *95*, 132–142. https://doi.org/10.1016/j.envsoft.2017.06.021

Lau, J., Butler, D., & Schütze, M. (2002). Is combined sewer overflow spill frequency/volume a good indicator of receiving water quality impact? *Urban Water*, *4*(2), 181–189. https://doi.org/10.1016/S1462-0758(02)00013-4

Li, C., Fletcher, T. D., Duncan, H. P., & Burns, M. J. (2017). Can stormwater control measures restore altered urban flow regimes at the catchment scale? *Journal of Hydrology*, *549*, 631–653. https://doi.org/10.1016/j.jhydrol.2017.03.037

Lim, T. C., & Welty, C. (2017). Effects of spatial configuration of imperviousness and green infrastructure networks on hydrologic response in a residential sewershed. *Water Resources Research*, *53*(9), 8084–8104. https://doi.org/10.1002/2017WR020631

Lim, T. C., & Welty, C. (2018). Assessing variability and uncertainty in green infrastructure planning using a high-resolution surface-subsurface hydrological model and site-monitored flow data. *Frontiers in Built Environment*, *4*(December), 1–15. https://doi.org/10.3389/fbuil.2018.00071

Lucas, W. C., & Sample, D. J. (2015). Reducing combined sewer overflows by using outlet controls for Green Stormwater Infrastructure: Case study in Richmond, Virginia. *Journal of Hydrology*, *520*, 473–488. https://doi.org/10.1016/j.jhydrol.2014.10.029

Mailhot, A., Talbot, G., & Lavallée, B. (2015). Relationships between rainfall and Combined Sewer Overflow (CSO) occurrences. *Journal of Hydrology*, *523*, 602–609. https://doi.org/10.1016/j.jhydrol.2015.01.063

Northeast Regional Climate Center. (2020). Evoporation Stations. Retrieved January 15, 2020, from http://www.nrcc.cornell.edu/wxstation/pet/pet.html

Pálfy, T. G., Molle, P., Langergraber, G., Troesch, S., Gourdon, R., & Meyer, D. (2016). Simulation of constructed wetlands treating combined sewer overflow using HYDRUS/CW2D. *Ecological Engineering*, *87*, 340–347. https://doi.org/10.1016/j.ecoleng.2015.11.048

Palla, A., & Gnecco, I. (2015). Hydrologic modeling of Low Impact Development systems at the urban catchment scale. *Journal of Hydrology*, *528*, 361–368. https://doi.org/10.1016/j.jhydrol.2015.06.050

Pennino, M. J., McDonald, R. I., & Jaffe, P. R. (2016). Watershed-scale impacts of stormwater green infrastructure on hydrology, nutrient fluxes, and combined sewer overflows in the mid-Atlantic region. *Science of the Total Environment*, *565*, 1044–1053. https://doi.org/10.1016/j.scitotenv.2016.05.101

Philadelphia Water Department. (2018). *Combined Sewer Management Program Annual Report*. Retrieved from http://archive.phillywatersheds.org/what_were_doing/documents_and_data/CSO_SW_AnnualReports

Reggiani, P., Sivapalan, M., & Hassanizadeh, S. M. (2000). Conservation equations governing hillslope responses: Exploring the physical basis of water balance. *Water Resources Research*, *36*(7), 1845–1863. https://doi.org/10.1029/2000WR900066

Robinson, J. S., & Sivapalan, M. (1997). Temporal scales and hydrological regimes: Implications for flood frequency scaling. *Water Resources Research*, *33*(12), 2981–2999. https://doi.org/10.1029/97WR01964

Rossman, L. a. (2015). *Storm Water Management Model User's Manual Version 5.1*. *United States Environment Protection Agency*. Washington, D.C. https://doi.org/PNR61

Schroeder, K., Riechel, M., Matzinger, A., Rouault, P., Sonnenberg, H., Pawlowsky-Reusing, E., & Gnirss, R. (2011). Evaluation of effectiveness of combined sewer overflow control measures by operational data. *Water Science & Technology*, *63*(2), 325. https://doi.org/10.2166/wst.2011.058

Seattle Public Utilities. (2019). *Wastewater Collection System: 2018 Annual Report*. Retrieved from http://www.seattle.gov/Documents/Departments/SPU/EnvironmentConservation/2018AnnualWastewaterCollectionSystemReport.pdf

Sebti, A., Fuamba, M., Bennis, S., Ph, D., Bennis, S., & Ph, D. (2016). Optimization model for BMP selection and placement in a combined sewer. *Journal of Water Resources Planning and Management*, *142*(3), 04015068. https://doi.org/10.1061/(ASCE)WR.1943-5452.0000620

Seo, Y., Schmidt, A. R., & Sivapalan, M. (2012). Effect of storm movement on flood peaks : Analysis framework based on characteristic timescales. *Water Resources Research*, *48*(March), 1–12. https://doi.org/10.1029/2011WR011761

Shuster, W., & Rhea, L. (2013). Catchment-scale hydrologic implications of parcel-level stormwater management (Ohio USA). *Journal of Hydrology*, *485*, 177–187. https://doi.org/10.1016/j.jhydrol.2012.10.043

Strupczewski, W., & Kundzewicz, Z. (1980). Muskingum method revisited. *Journal of Hydrology*, *48*(3–4), 327–342. https://doi.org/10.1016/0022-1694(80)90124-9

Tavakol-Davani, H., Goharian, E., Hansen, C. H., Tavakol-Davani, H., Apul, D., & Burian, S. J. (2016). How does climate change affect combined sewer overflow in a system benefiting from rainwater harvesting systems? *Sustainable Cities and Society*, *27*, 430–438. https://doi.org/10.1016/j.scs.2016.07.003

Troch, P. A., Carrillo, G. A., Heidbüchel, I., Rajagopal, S., Switanek, M., Volkmann, T. H. M., & Yaeger, M. (2009). Dealing with landscape heterogeneity in watershed hydrology: A review of recent progress toward new hydrological theory. *Geography Compass*, *3*(1), 375–392. https://doi.org/10.1111/j.1749-8198.2008.00186.x

USEPA. (2011). *Keeping raw sewage and contaminated stormwater out of the public's water*. New York, NY.

Wagener, T., Sivapalan, M., Troch, P. A., McGlynn, B. L., Harman, C. J., Gupta, H. V., … Wilson, J. S. (2010). The future of hydrology: An evolving science for a changing world. *Water Resources Research*, *46*(5), 1–10. https://doi.org/10.1029/2009WR008906

Wagener, T., Sivapalan, M., Troch, P., & Woods, R. (2007). Catchment classification and hydrologic similarity. *Geography Compass*, *1*(4), 901–931. https://doi.org/10.1111/j.1749-8198.2007.00039.x

Western Regional Climate Center. (2020). Potential Evapotranspiration for Selected Locations. Retrieved January 15, 2020, from

https://wrcc.dri.edu/Climate/comp_table_show.php?stype=pan_evap_avg
Wood, E. F., & Hebson, C. S. (1986). On hydrologic similarity: 1. Derivation of the simensionless flood frequency curve. *Water Resources Research*, *22*(11), 1549–1554. https://doi.org/10.1029/WR022i011p01549
Woods, R., & Sivapalan, M. (1999). A synthesis of space-time variability in storm response: Rainfall, runoff generation, and routing. *Water Resources Research*, *35*(8), 2469–2485. https://doi.org/10.1029/1999WR900014

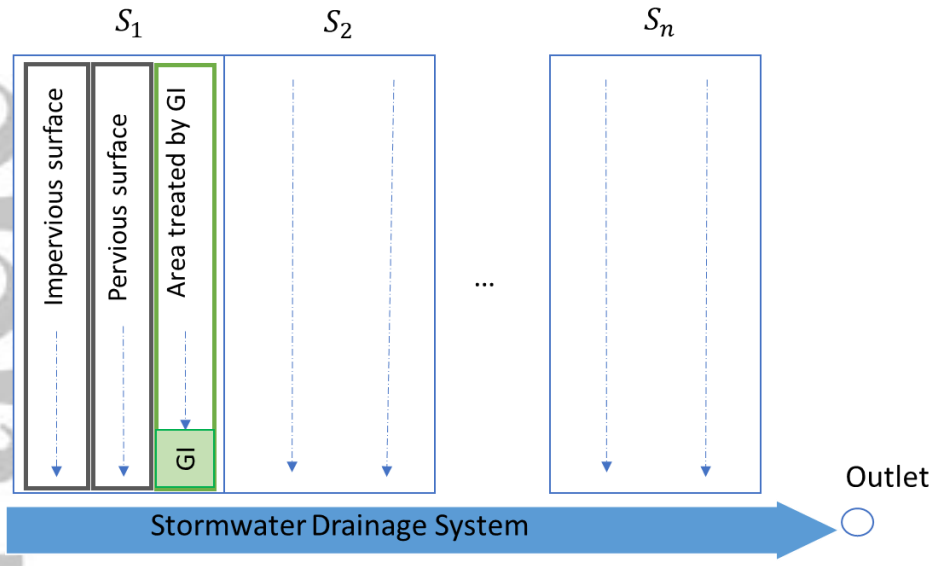

Figure 1. Urban sewershed representation with n subsewersheds, S_1, S_2,…, and S_n, where each subsewershed is divided into impervious, pervious and area treated by GI

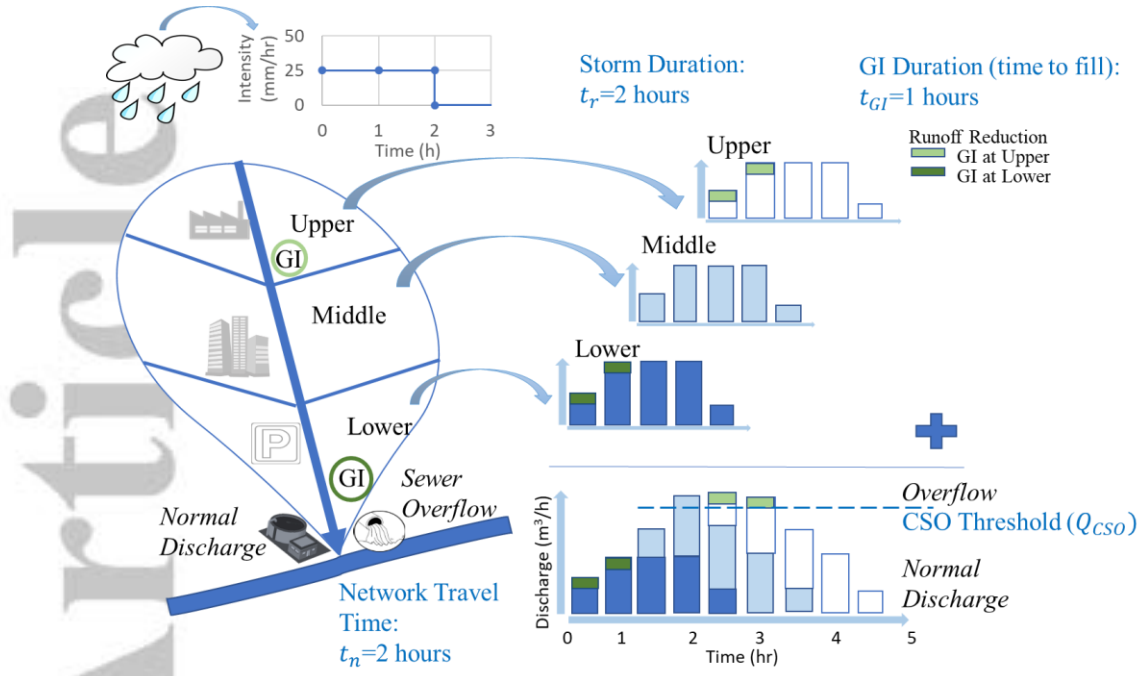

Figure 2. Conceptual diagram of the effect of GI on an urban sewershed and the resulting hydrographs for an idealized sewershed with GI at Upper and Lower subsewersheds, given a uniform rainfall with an intensity of 25.4 mm/h for two hours. Hydrograph bars each have a width of 0.5 h; travel time of flows from the Upper to Middle and then Middle to the sewershed outfall are each 1 h. The runoff reduction by GIs shown by the light green and dark green boxes on the hydrographs, represent the reduction at Upper and Lower subsewersheds, respectively.

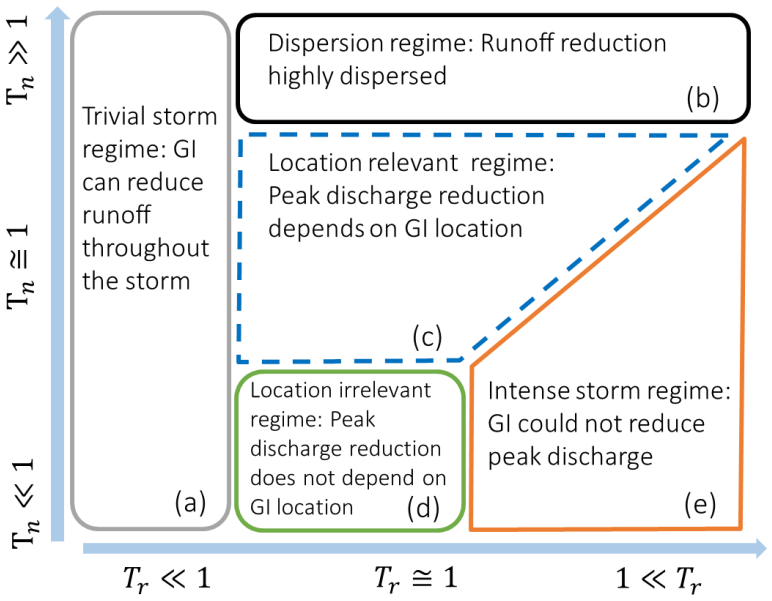

Figure 3. Peak discharge regimes identified by the dimensionless timescales in $\boldsymbol{T_r}$-$\boldsymbol{T_n}$ space

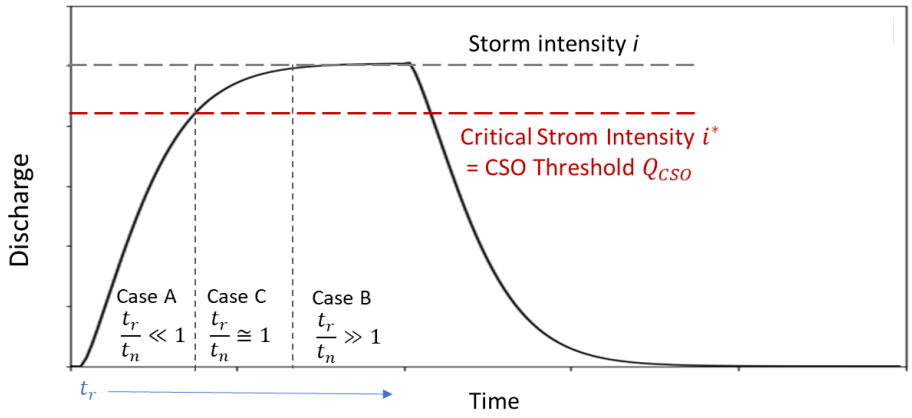

Figure 4. The three cases of $\frac{t_r}{t_r}$, the maximum storm intensity and the critical storm intensity triggering CSO in a hydrograph during a uniform storm event

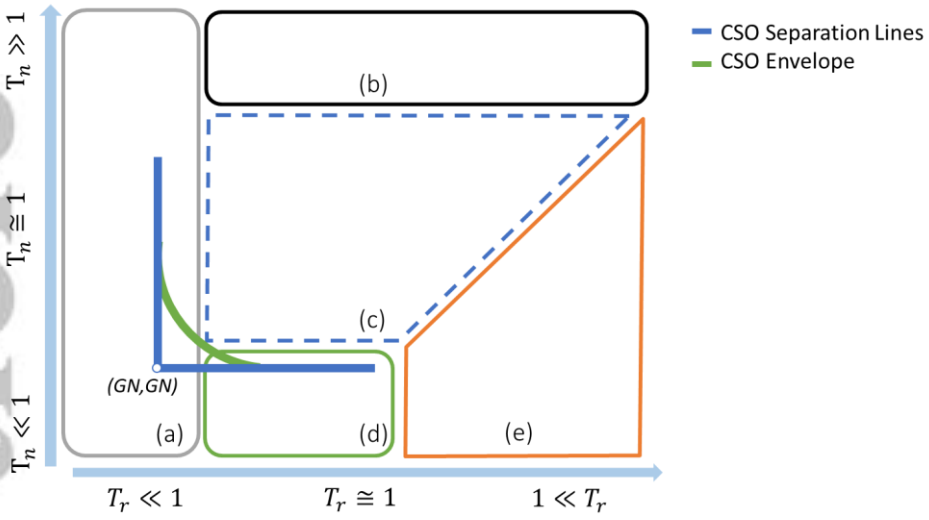

Figure 5. The timescale framework for stormwater management with GI where the colored outlines are the peak discharge regimes identified in Section 2.3, the blue lines are the *CSO Separation Lines* and the green line is the *CSO Envelope*.

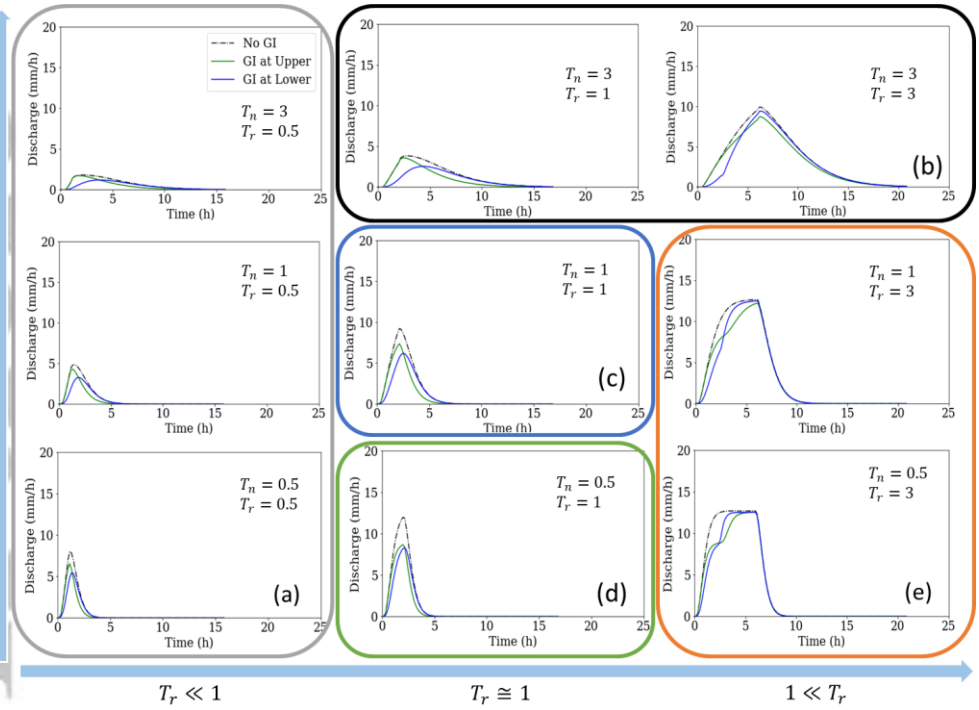

Figure 6. Hydrographs showing the response of the hypothetical sewersheds with GI at the Lower and Upper subsewersheds with various combinations of T_r and T_n values under uniform storms (i = 12.7 mm/h; $\boldsymbol{t_r} = \boldsymbol{t_{GI}} * T_r = 2T_r$). The green and blue lines in the subplots show the discharge with GI at the Upper and Lower subsewersheds, respectively, and the black dash lines indicate the discharge without GI. The subplots are arranged corresponding to the peak discharge regimes identified in Figure 3, where T_r increases from left to right and T_n increases from bottom to top.

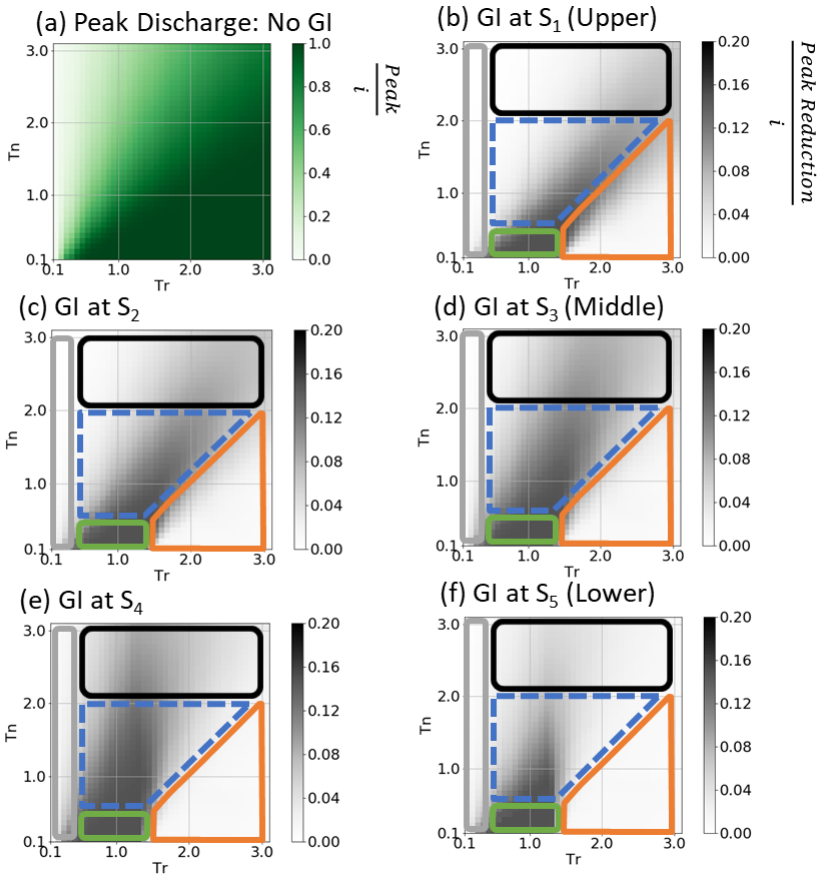

Figure 7. The peak discharge of hypothetical sewersheds without GI (a) and the peak discharge reduction with GI at S_1 (b), S_2 (c), S_3 (d), S_4 (e), and S_5 (f) under various $\boldsymbol{T_r}$-$\boldsymbol{T_n}$ combinations with the peak discharge regimes imposed on each subfigure

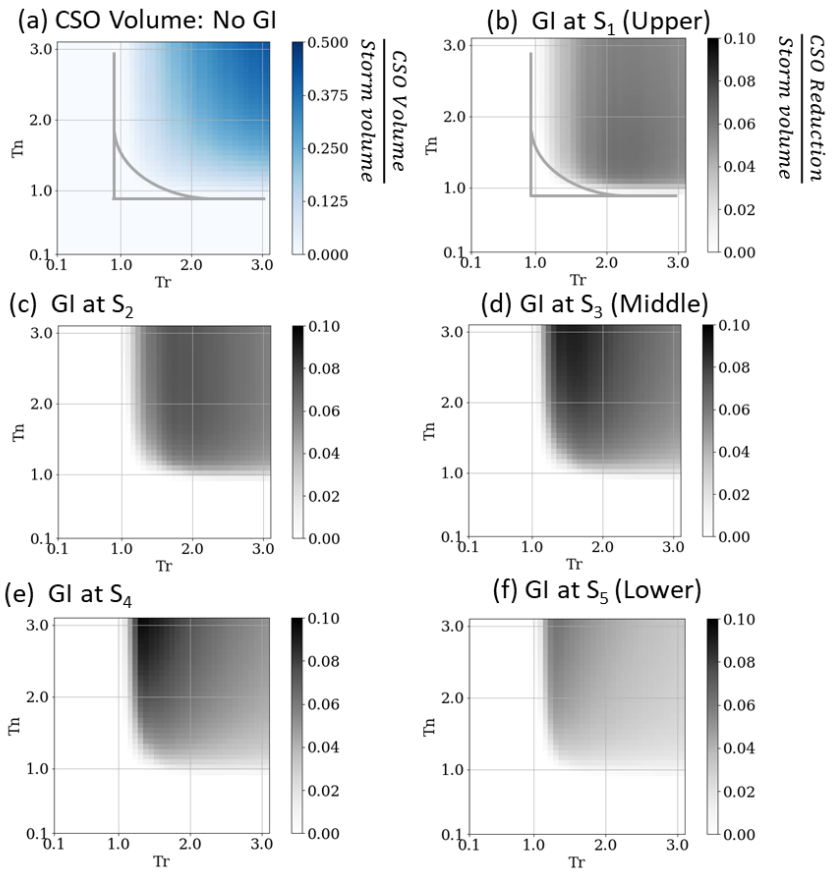

Figure 8. The CSO generation of a hypothetical sewershed without GI (a) and the volume reduction with GI at S_1 (b), S_2 (c), S_3 (d), S_4 (e), and S_5 (f) with combinations of $\boldsymbol{T_r}$ and $\boldsymbol{T_n}$ ($\boldsymbol{Q_{cso}}$= 7.62 mm/h); the CSO separation lines and the envelope curve are imposed on (a) and (b) which outlines the regions with CSOs that could be managed by GI

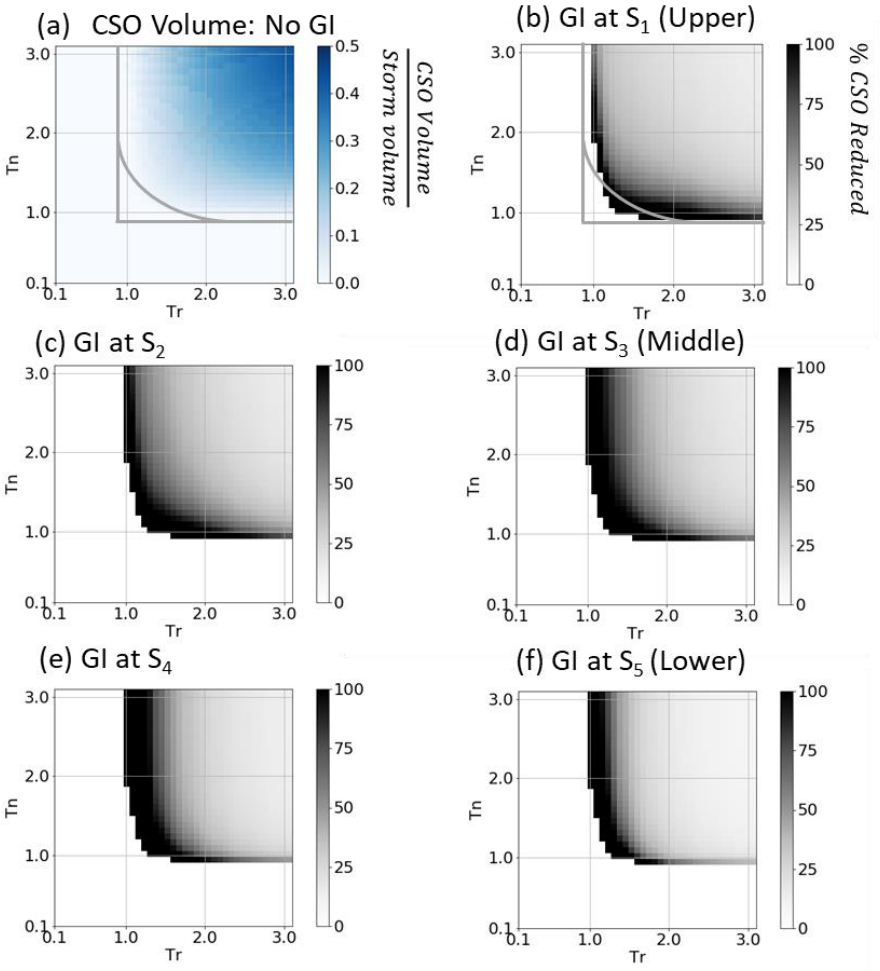

Figure 9. The CSO volume normalized by total storm volume of a hypothetical sewershed without GI (a) and the volume reduction with GI at S_1 (b), S_2 (c), S_3 (d), S_4 (e), and S_5 (f) normalized by the total CSO volume (in %); the CSO separation lines and the envelope curve are imposed on (a) and (b) to indicate the area where CSOs can be eliminated.

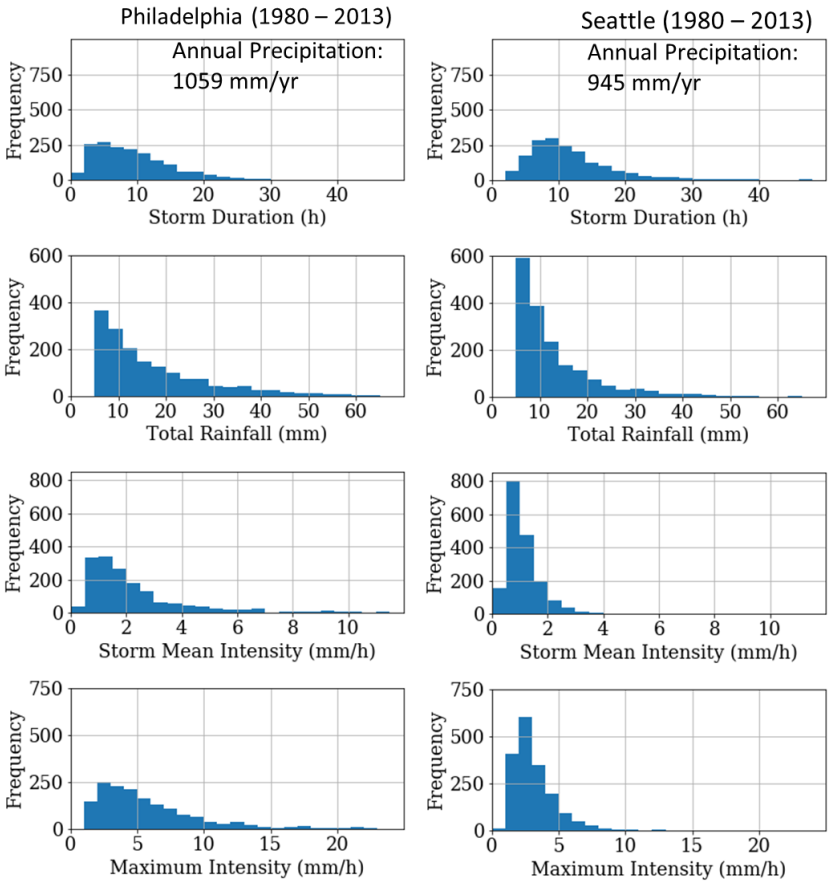

Figure 10. The histograms of the storm duration, the storm mean intensity, the total volume, and the maximum intensity in Philadelphia and Seattle. Note that small storms with total rainfall below 5 mm are removed so that differences in the storm characteristics of the two data sets are more evident.

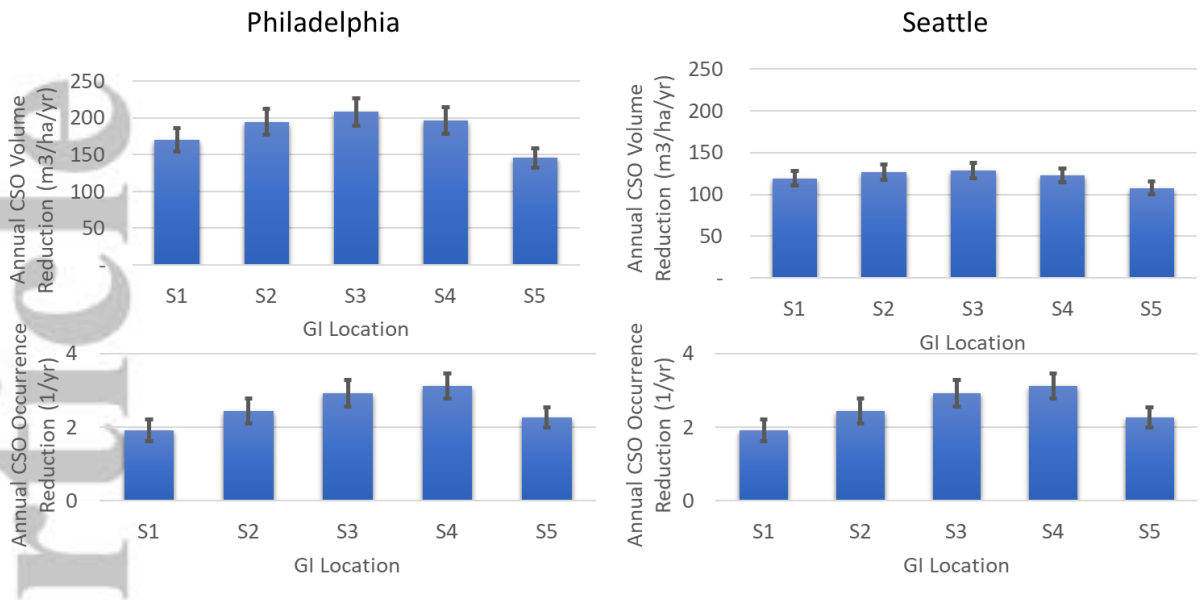

Figure 11. Annual CSO volume and occurrence reductions with GI at each subsewershed on the hypothetical sewershed in Philadelphia and Seattle. Note: the average annual CSO volume and occurrence without GI are 740 m^3/ha/yr and 8.3 CSO/yr in Philadelphia and 390 m^3/ha/yr and 8.6 CSO/yr in Seattle.

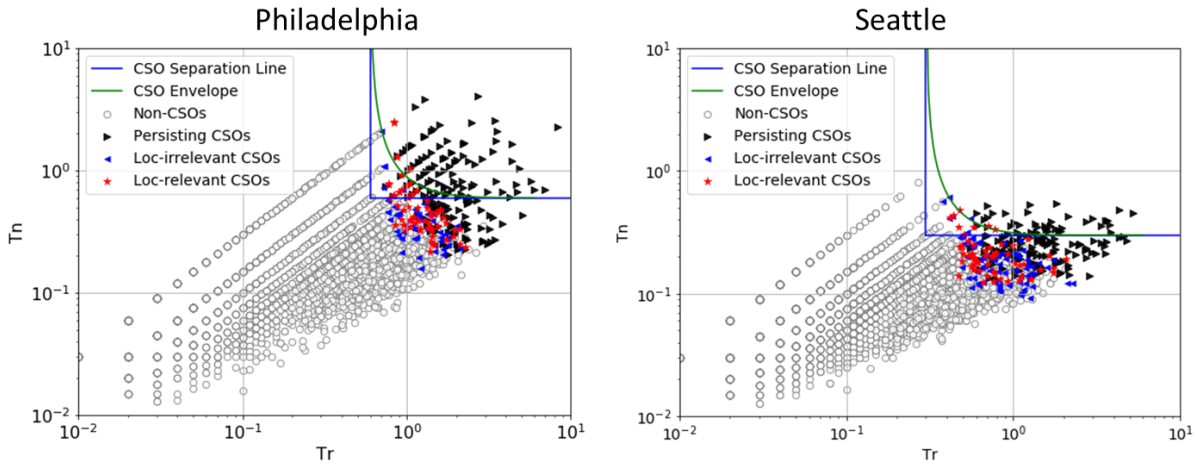

Figure 12. The scatter plots of the storms from 1980 to 2013 in Philadelphia and Seattle on a hypothetical sewershed with $\boldsymbol{t_n} = 3$ hours, and the approximation of the CSO separation lines and the CSO envelope curve in Log T_r-T_n Space.

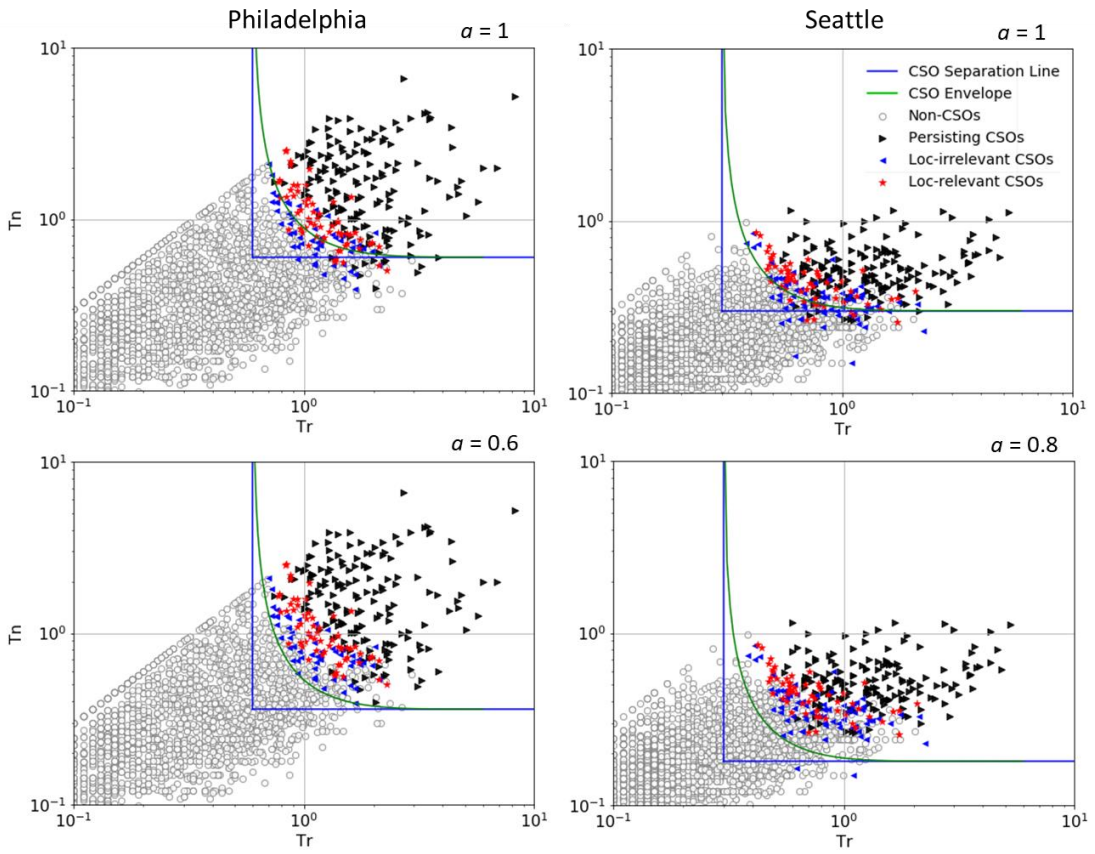

Figure 13. The adjusted scatter plots of the storms in Philadelphia and Seattle on a hypothetical sewershed where the critical intensity is the 90%-quantile intensity, and the adjustment factors (0.6 and 0.8 for Philadelphia and Seattle, respectively) are applied to shift the CSO separation lines and the envelopes down

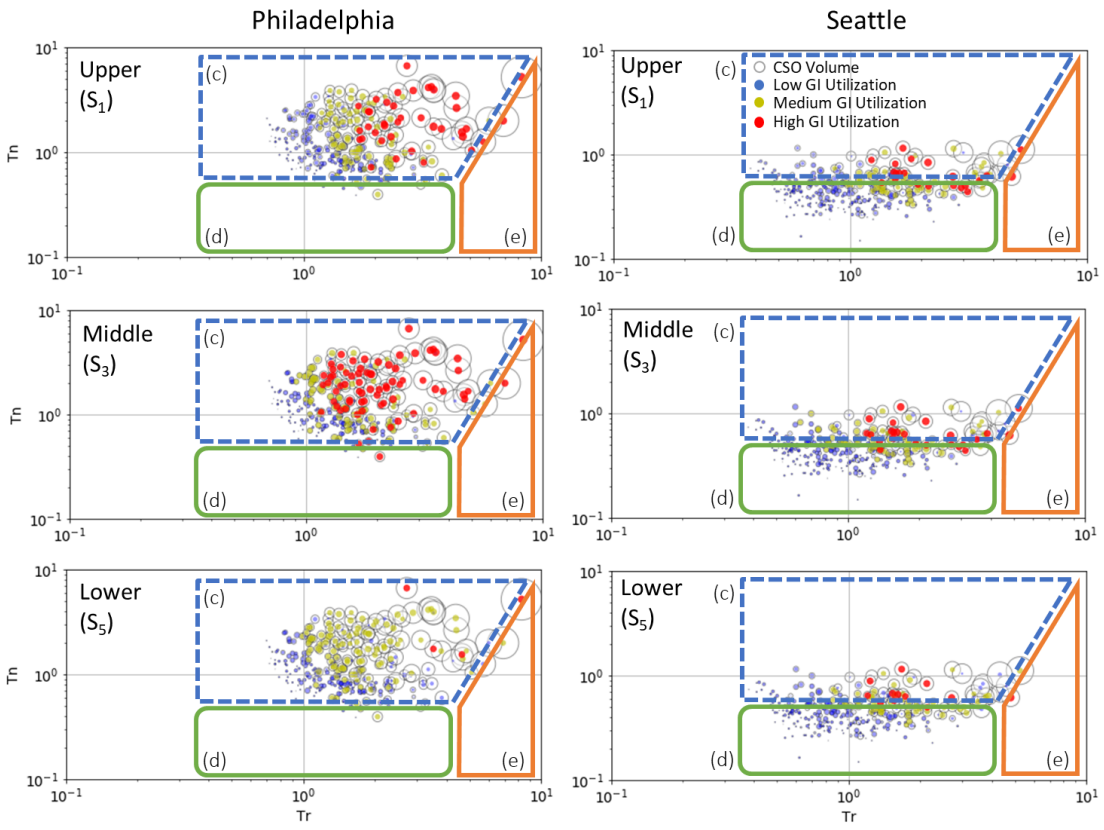

Figure 14. CSO storms in the 34-years data in T_r -T_n space, where the areas of the circles represent the magnitude of the CSO volume and the reductions achieved by siting GI in the Upper (S_1), Middle (S_3), and Lower (S_5) subsewersheds. The total CSO volume (without GI) is the hollow circle area outlined in gray, while the reductions due to the installation of GI are stacked on the hollow circles and colored into three categories: blue for low (0, 40%), yellow for medium (40%,80%) and red for high (80%,100%) GI storage utilizations. In addition, the outline of the peak discharge regimes excluding Figure 3a and 3b is stacked on each subfigure to show the focal point for the GI location effect. The results of siting GI at S_2 and S_4 are intermediate to the adjoining cases, so we only show the results of the simulation with GI at the Upper (S_1), Middle (S_3), and Lower (S_5) subsewersheds for brevity.

Table 1. The number of years (out of 34) that GI sited at each subsewershed provides the highest and the lowest annual CSO volume reduction and the corresponding fraction

	Philadelphia				**Seattle**			
	Highest Reduction		Lowest Reduction		Highest Reduction		Lowest Reduction	
	Count	*Prob.*	*Count*	*Prob.*	*Count*	*Prob.*	*Count*	*Prob.*
S1	0	0%	9	26%	1	3%	7	21%
S2	4	12%	0	0%	9	26%	0	0%
S3	26	76%	0	0%	20	59%	0	0%
S4	4	12%	0	0%	4	12%	0	0%
S5	0	0%	25	74%	0	0%	27	79%
Sum	34	100%	34	100%	34	100%	34	100%